αvβ3- and αvβ5-integrins on the cell membrane [5,29]. Therefore, we examined the expression of CAR, αv-integrin, β3-integrin and β5-integrin in human and rat trophoblast cell lines by RT–PCR analysis. Total RNA was isolated using TRIZOL reagent (Life Technologies, Tokyo, Japan). Reverse transcription (RT) was performed using a TaKaRa RNA PCR kit (AMV) Ver. 2.1 for first strand cDNA synthesis (TaKaRa Bio, Osaka, Japan) according to the instructions of the manufacturer. After the RT reaction, the rat/human CAR and integrins (αv, β3 and β5) were amplified by PCR. The primers and the expected size of the PCR product are summarized in Table 2. PCR conditions were as follows: human CAR, 30 s at 94 °C, 60 s at 65 °C, and 120 s at 72 °C for 30 cycles; human αv-integrin, 40 s at 94 °C, 60 s at 65 °C, and 120 s at 72 °C for 40 cycles; human β3-integrin, 30 s at 94 °C, 40 s at 65 °C, and 60 s at 72 °C for 30 cycles; human β5-integrin, 40 s at 94 °C, 40 s at 58 °C, and 60 s at 72 °C for 20 cycles; human β-actin, 30 s at 94 °C, 30 s at 60 °C, and 30 s at 72 °C for 35 cycles; rat CAR, 45 s at 94 °C, 60 s at 53 °C, and 90 s at 72 °C for 40 cycles; rat αv-integrin, 45 s at 94 °C, 60 s at 57 °C, and 90 s at 72 °C for 30 cycles; rat β3-integrin, 45 s at 94 °C, 60 s at 58 °C, and 90 s at 72 °C for 30 cycles; rat β5-integrin, 45 s at 94 °C, 60 s at 53 °C, and 90 s at 72 °C for 40 cycles; and rat glyceraldehyde-3-phosphate dehydrogenase (GAPDH), 45 s at 94 °C, 60 s at 60 °C, and 90 s at 72 °C for 40 cycles.

PCR products were electrophoresed in a 2.0% agarose gel. To ensure the quality of the procedure, RT–PCR was also performed using specific primers for β-actin and GAPDH.

Statistical analysis

The significant difference was calculated using one-way ANOVA followed by Dunnett's test.

RESULTS

Human trophoblast cells

As shown in Figure 1, CAR and αv-integrin were expressed in all of the trophoblast cell lines. β3-Integrin expression was not detected in JEG-3 cells, and β5-integrin expression was not observed in BeWo cells.

Next, we compared the efficacy of gene transfer mediated by Ad-L2, Ad-RGD(HI)-L2, Ad-K7(C)-L2 and Ad-RGD(HI)K7(C)-L2 vectors in three cell lines, JAR, JEG-3 and BeWo. Although every combination of vector and cell line resulted in luciferase production, the amount of luciferase varied markedly (Figure 2). The greatest amount of luciferase was produced by the Ad-RGD(HI)-L2 vector. When compared to Ad-L2, Ad-RGD(HI)-L2 mediated the production of 8.1-fold the amount of luciferase in JEG-3 cells, 13.5-fold the amount in JAR cells, and 76.8-fold the amount in BeWo cells. The second highest amounts of luciferase were mediated by the Ad-RGD(HI)K7(C)-L2 vector. When compared to Ad-L2, Ad-RGD(HI)K7(C)-L2 mediated the production of 4.2-fold the amount of luciferase in JAR cells, 6.2-fold in JEG-3 cells, and 9.4-fold in BeWo cells. Modification of K7 in the fiber knob domain did not result in increased luciferase production in JAR cells and JEG-3

Table 2. Primers for RT–PCR analysis

Gene		Sequence (5′ to 3′)	Parameter (°C)	Expected size (bp)
Human CAR	Forward	AGCCTTCAGGTGCGAGATGTTACG	65	366
	Reverse	TAGGACAGCAAAAGATGATAAGAC		
Human αv-integrin	Forward	GCCTATCTCCACGCACACTG	65	287
	Reverse	TTGGACCATTGTTTCTCAGC		
Human β3-integrin	Forward	GAGGATGACTGTGTCGTCAG	65	232
	Reverse	CTGGCGCGTTCTTCCTCAAA		
Human β5-integrin	Forward	GCCTATCTCCACGCACACTG	58	454
	Reverse	AGACTCCGACCCTTCCTGAC		
Human β-actin	Forward	CAAGAGATGGCCACGGCTGCT	60	275
	Reverse	TCCTTCTGCATCCTGTCGGCA		
Rat CAR	Forward	ATGGATCCTACACCCGAACAGAGGATCG	53	280
	Reverse	GCGAATTCGCGTCGCCAGACTTGACAT		
Rat αv-integrin	Forward	GCCTATCTCCACGCACACTG	57	273
	Reverse	CGGGTGCTATCTGTCTTATG		
Rat β3-integrin	Forward	TAATGATGGGCGCTGCCACA	58	279
	Reverse	CGTAAGCATCAACGATGAGC		
Rat β5-integrin	Forward	TGTGTCTCTGCGGTGTTTGC	53	312
	Reverse	CCACGAGAACACCACAACAA		
Rat GAPDH	Forward	ACCACAGTCCATGCCATCAC	60	452
	Reverse	TCCACCACCCTGTTGCTGTA		

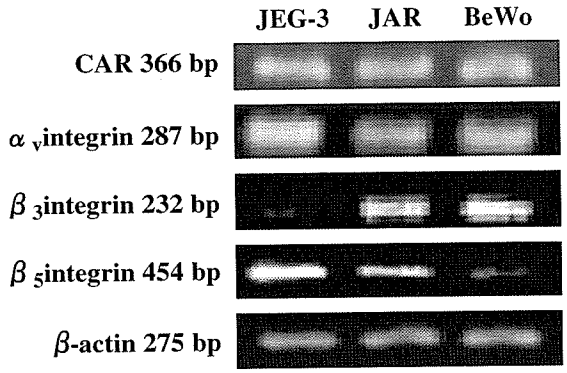

Figure 1. RT–PCR analysis of CAR and integrin (αv, β3, β5) and β-actin expression in human trophoblast cell lines.

cells. But, as compared to Ad-L2 vector, the modification of K7 elevated the luciferase production by 4.6-fold in BeWo cells.

Rat trophoblast cells

Next, we investigated the effects of different Ad vectors on transgene expression in Rcho-1 cells and TR-TBT (18d-1 and

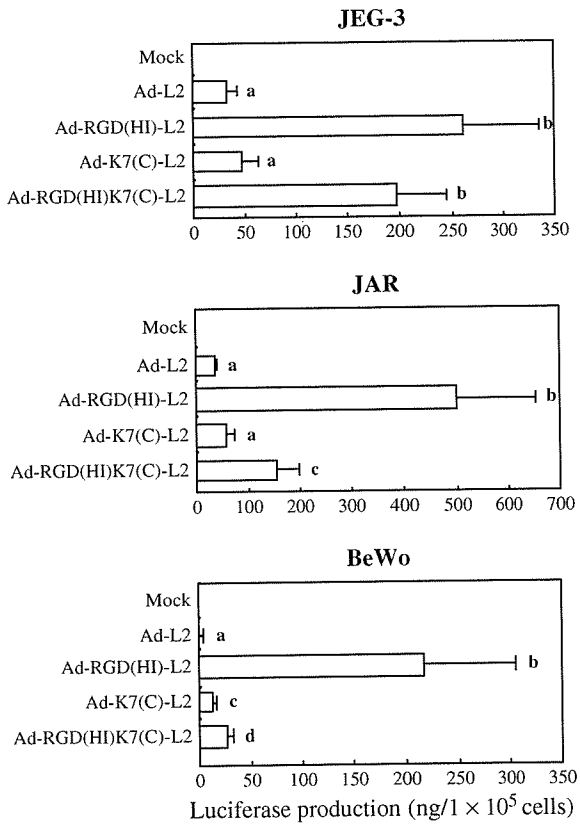

Figure 2. Luciferase production in human trophoblast cell lines transduced by Ad-L2, Ad-RGD(HI)-L2, Ad-K7(C)-L2 or Ad-RGD(HI)-K7(C)-L2. Cells were transduced with 300 vector particles per cell for 1.5 h. A luminescent assay was used to measure luciferase production after 48 h of culture. Data are expressed as mean ± S.D. ($n = 4$). Significant difference is observed among the groups with different letters ($p < 0.01$).

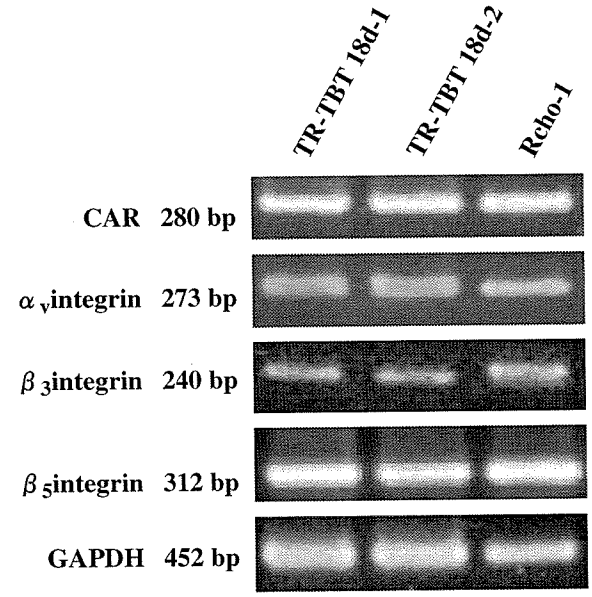

Figure 3. RT–PCR analysis of CAR and integrin (αv, β3, β5) and GAPDH expression in rat trophoblast cell lines.

18d-2) cells. RT–PCR analysis revealed that mRNA for CAR, αv-integrin, β3-integrin and β5-integrin is expressed in each rat trophoblast cell line (Figure 3). We studied the gene transfer activities mediated by the Ad-RGD(HI), Ad-K7(C)-L2 and Ad-RGD(HI)K7(C)-L2 vectors in rat trophoblast cell lines. When compared to Ad-L2 vector, Ad-RGD(HI)-L2 mediated the production of 5–20 times more luciferase (Figure 4). Ad-K7(C)-L2 caused decreased luciferase production when compared to Ad-L2 vectors (34% in Rcho-1, 43% in TR-TBT 18d-1 and 56% in TR-TBT 18d-2). Ad-RGD(HI)K7(C)-L2-mediated gene transfer resulted in increased luciferase production when compared with Ad-L2 vectors, but the production of luciferase was lower than that mediated by Ad-RGD(HI)-L2.

DISCUSSION

The first step in Ad infection is the binding of the fiber knob of Ad with CAR on the cell membrane [5,6]. Since the HI loop and C-terminus of the fiber are not involved in formation of the CAR-binding site [30–32], we developed fiber-modified Ad vectors with expanded tropism by insertion of the RGD motif and/or K7 motif into the HI loop and/or the C-terminus of the fiber [12,15,33]. In the present study, we evaluated the ability of several fiber-modified Ad vectors to transduce human and rat trophoblast cell lines. We found that Ad-RGD(HI) vector, which contains an RGD motif in the fiber knob, is the prominent vector system for transduction of human and rat trophoblast cell lines.

In human trophoblast cell lines, Ad-RGD(HI)-L2 was the most efficient vector, Ad-RGD(HI)K7(C)-L2 had moderate efficiency, and Ad-K7(C)-L2 and Ad-L2 were the least

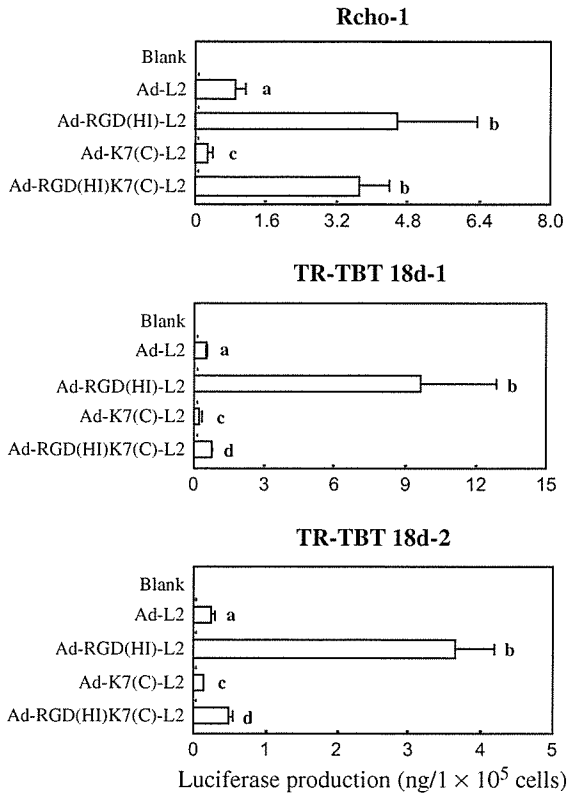

Figure 4. Luciferase production in rat trophoblast cells transduced by Ad-L2, Ad-RGD(HI)-L2, Ad-K7(C)-L2 or Ad-RGD(HI)-K7(C)-L2. Cells were transduced with 300 vector particles per cell for 1.5 h. A luminescent assay was used to measure luciferase production after 48 h of culture. Data are expressed as mean ± S.D. ($n = 4$). Significant difference is observed among the groups with different letters ($p < 0.01$).

efficient. Although Ad-K7(C)-L2 mediated greater luciferase production than Ad-L2 in JAR and BeWo cells, the transgene effects of Ad-RGD(HI)K7(C)-L2 were weak (rather than additive) when compared to Ad-RGD(HI)-L2 and Ad-K7(C)-L2. The RGD motif contains a positively charged arginine (R) residue. Thus, the lower efficiency of Ad-RGD(HI)K7(C)-L2 vector may be caused by a disturbance in the interaction of the fiber with the ligand on the membrane by the positively charged K7 motif in JAR and BeWo cells. In spite of the absence of β3-integrin expression, the transgene effect of Ad-RGD(HI)-L2 was observed in JEG-3 cells. We found that expression of β3-integrin was not responsible for transgene activity of Ad-RGD(HI)-L2 in mouse fibroblast L cells and human glioma LN444 cells [12]. So, Ad-RGD(HI)-L2 in JEG-3 may infect JEG-3 cells via an αvβ5-integrin-dependent pathway. Ad-RGD(HI)-L2 was also the most promising vector for transgene expression in rat trophoblast cell lines. The transducing efficiency in rat trophoblast cell lines was not increased by the insertion of the K7 motif in the fiber knob. This suggests that interaction between heparan sulfate on the cell membrane and the fiber containing the K7 motif did not contribute to infection with Ad vector. The lower transgene efficiency mediated by the insertion of the RGD motif and K7 motif in the knob of the fiber (as compared to the insertion of only the RGD motif) may be caused by positively charged K7 disturbing the interaction between the RGD motif and integrin. Dmitriev et al. [8] reported that the RGD motif of the penton base of Ad does not contribute to the binding to αvβ3-integrin on the cell membrane. Ad-RGD(HI) may effectively infect trophoblast cells in the RGD motif in a fiber-dependent fashion.

In summary, fiber-modified Ad that contains the RGD motif in the fiber knob is a promising vector for gene transfer to human and rat trophoblast cell lines. This is the first report to compare the gene transfer activity of various recombinant Ad vectors in trophoblast cell lines. Our findings will be useful for future clinical and basic research regarding the placenta.

ACKNOWLEDGEMENT

We thank Dr. M. J. Soares (University of Kansas Medical Center) for kindly providing us Rcho-1 cells. This work was supported by a Grants-in-Aid for Scientific Research (C) (No. 15590139) from the Ministry of Education, Culture, Sports, Science and Technology, Japan.

REFERENCES

[1] Parry S, Koi H, Strauss III JF. Transplacental drug delivery: gene and virus delivery to the trophoblast. Adv Drug Deliv Rev 1999;38: 69–80.

[2] MacCalman CD, Furth EE, Omigbodun A, Kozarsky KF, Coutifaris C, Strauss III JF. Transduction of human trophoblast cells by recombinant adenovirus is differentiation dependent. Biol Reprod 1996;54:682–91.

[3] Koi H, Zhang J, Makrigiannakis A, Getsios S, MacCalman CD, Kopf GS, et al. Differential expression of the coxsackievirus and adenovirus receptor regulates adenovirus infection of the placenta. Biol Reprod 2001;64:1001–9.

[4] Parry S, Holder J, Halterman MW, Weitzman MD, Davis AR, Federoff H, et al. Transduction of human trophoblastic cells by replication deficient recombinant viral vectors. Am J Pathol 1998;152: 1521–9.

[5] Bergelson JM, Cunningham JA, Droguett G, Kurt-Jones EA, Krithivas A, Hong JS, et al. Isolation of a common receptor for coxsackie B viruses and adenoviruses 2 and 5. Science 1997;275:1320–3.

[6] Tomko RP, Xu R, Philipson L. HCAR and MCAR: the human and mouse cellular receptors for subgroup C adenoviruses and group B coxsackieviruses. Proc Natl Acad Sci U S A 1997;94:3352–6.

[7] Wickham TJ, Tzeng E, Shears 2nd LL, Roelvink PW, Li Y, Lee GM, et al. Increased in vitro and in vivo gene transfer by adenovirus vectors containing chimeric fiber proteins. J Virol 1997;71:8221–9.

[8] Dmitriev I, Krasnykh V, Miller CR, Wang M, Kashentseva E, Mikheeva G, et al. An adenovirus vector with genetically modified fibers demonstrates expanded tropism via utilization of a coxsackievirus. J Virol 1998;72:9706–13.

[9] Hidaka C, Milano E, Leopold PL, Bergelson JM, Hackett NR, Finberg RW, et al. CAR-dependent and CAR-independent pathways of adenovirus vector-mediated gene transfer and expression in human fibroblasts. J Clin Invest 1999;4:579–87.

[10] Staba MJ, Wickham TJ, Kovesdi I, Hallahan DE. Modifications of the fiber in adenovirus vectors increase tropism for malignant glioma models. Cancer Gene Ther 2000;7:13–9.

[11] Hay CM, De Leon H, Jafari JD, Jakubczak JL, Mech CA, Hallenbeck PL, et al. Enhanced gene transfer to rabbit jugular veins by

an adenovirus containing a cyclic RGD motif in the HI loop of the fiber knob. J Vasc Res 2002;38:315–23.

[12] Koizumi N, Mizuguchi H, Hosono T, Ishii-Watabe A, Uchida E, Utoguchi N, et al. Efficient gene transfer by fiber-mutant adenoviral vectors containing RGD peptide. Biochem Biophys Acta 2001;1568: 13–20.

[13] Okada N, Tsukada Y, Nakagawa S, Mizuguchi H, Mori K, Saito T, et al. Efficient gene delivery into dendritic cells by fiber-mutant adenovirus vectors. Biochem Biophys Res Commun 2001;282:173–9.

[14] Mizuguchi H, Koizumi N, Hosono T, Utoguchi N, Watanabe Y, Kay MA, et al. A simplified system for constructing recombinant adenoviral vectors containing heterologous peptides in the HI loop of their fiber knob. Gene Ther 2001;8:730–5.

[15] Koizumi N, Mizuguchi H, Utoguchi N, Watanabe Y, Hayakawa T. Generation of fiber-modified adenovirus vectors containing heterologous peptides in both the HI loop and C terminus of the fiber knob. J Gene Med 2003;5:267–76.

[16] Bouri K, Feero WG, Myerburg MM, Wickham TJ, Kovesdi I, Hoffman EP, et al. Poly-lysine modification of adenoviral fiber protein enhances muscle cell transduction. Hum Gene Ther 1999;10: 1633–40.

[17] Gonzalez R, Vereecque R, Wickham TJ, Facon T, Hetuin D, Kovesdi I, et al. Transduction of bone marrow cells by the AdZ.F(pK7) modified adenovirus demonstrates preferential gene transfer in myeloma cells. Hum Gene Ther 1999;10:2709–17.

[18] Gonzalez R, Vereecque R, Wickham TJ, Vanrumbeke M, Kovesdi I, Bauters F, et al. Increased gene transfer in acute myeloid leukemic cells by an adenovirus vector containing a modified fiber protein. Gene Ther 1999;6:314–20.

[19] Wu H, Seki T, Dmitriev I, Uil T, Kashentseva E, Han T, et al. Double modification of adenovirus fiber with RGD and polylysine motifs improves coxsackievirus–adenovirus receptor-independent gene transfer efficiency. Hum Gene Ther 2002;13:1647–53.

[20] Yamamoto T, Roby KF, Kwok SC, Soares MJ. Transcriptional activation of cytochrome P450 side chain cleavage enzyme expression during trophoblast cell differentiation. J Biol Chem 1994;269:6517–23.

[21] Hamlin GP, Soares MJ. Regulation of deoxyribonucleic acid synthesis in proliferating and differentiating trophoblast cells: involvement of transferrin, transforming growth factor-β, and tyrosine kinases. Endocrinology 1995;136:322–31.

[22] Oda M, Sun W, Hattori N, Tanaka S, Shiota K. PAL31 expression in rat trophoblast giant cells. Biochem Biophys Res Commun 2001;287: 721–6.

[23] Ohgane J, Hattori N, Oda M, Tanaka S, Shiota K. Differentiation of trophoblast lineage is associated with DNA methylation and demethylation. Biochem Biophys Res Commun 2002;290:701–6.

[24] Kitano T, Iizasa H, Terasaki T, Asashima T, Matsunaga N, Utoguchi N, et al. Polarized glucose transporters and mRNA expression properties in newly developed rat syncytiotrophoblast cell lines, TR-TBTs. J Cell Physiol 2002;193:208–18.

[25] Mizuguchi H, Kay MA. Efficient construction of a recombinant adenovirus vector by an improved in vitro ligation method. Hum Gene Ther 1998;9:2577–83.

[26] Mizuguchi H, Kay MA. A simple method for constructing E1 and E1/E4 deleted recombinant adenovirus vector. Hum Gene Ther 1999;10: 2013–7.

[27] Maizel Jr JV, White DO, Scharff MD. The polypeptides of adenovirus. I. Evidence for multiple protein components in the virion and a comparison of types 2, 7A, and 12. Virology 1968;36:115–25.

[28] Kanegae Y, Makimura M, Saito I. A simple and efficient method for purification of infectious recombinant adenovirus. Jpn J Med Sci Biol 1994;47:157–66.

[29] Wickham TJ, Filardo EJ, Cheresh DA, Nemerow GR. Integrin αvβ5 selectively promotes adenovirus mediated cell membrane permeabilization. J Cell Biol 1994;127:257–64.

[30] Xia D, Henry LJ, Gerard RD, Deisenhofer J. Crystal structure of the receptor-binding domain of adenovirus type 5 fiber protein at 1.7 Å resolution. Structure 1994;2:1259–70.

[31] Kirby I, Davison E, Beavil AJ, Soh CP, Wickham TJ, Roelvink PW, et al. Modulation in the DG loop of adenovirus type 5 fiber knob protein abolish high-affinity binding to its cellular receptor CAR. J Virol 1999;73: 9508–14.

[32] Kirby I, Davison E, Beavil AJ, Soh CP, Wickham TJ, Roelvink PW, et al. Identification of contact residues and definition of the CAR-binding site of adenovirus type 5 fiber protein. J Virol 2000;74:2804–13.

[33] Mizuguchi H, Koizumi N, Hosono T, Ishii-Watabe A, Uchida E, Utoguchi N, et al. CAR- or alphav integrin-binding ablated adenovirus vectors, but not fiber-modified vectors containing RGD peptide, do not change the systemic gene transfer properties in mice. Gene Ther 2002;9: 769–76.

THE JOURNAL OF GENE MEDICINE
J Gene Med 2005; 7: 604–612.
Published online 15 November 2004 in Wiley InterScience (www.interscience.wiley.com). **DOI:** 10.1002/jgm.699

RESEARCH ARTICLE

PEGylated adenovirus vectors containing RGD peptides on the tip of PEG show high transduction efficiency and antibody evasion ability

Yusuke Eto[1†]
Jian-Qing Gao[1,2†]
Fumiko Sekiguchi[1]
Shinnosuke Kurachi[1]
Kazufumi Katayama[1]
Mitsuko Maeda[4]
Koichi Kawasaki[4]
Hiroyuki Mizuguchi[3]
Takao Hayakawa[3]
Yasuo Tsutsumi[3]
Tadanori Mayumi[4]
Shinsaku Nakagawa[1*]

[1]*Graduate School of Pharmaceutical Sciences, Osaka University, Japan*

[2]*College of Pharmaceutical Sciences, Zhejiang University, P.R. China*

[3]*National Institute of Health Sciences, Japan*

[4]*School of Pharmaceutical Sciences, Kobe Gakuin University, Japan*

*Correspondence to:
Shinsaku Nakagawa, Department of Biopharmaceutics, Graduate School of Pharmaceutical Sciences, Osaka University, Yamadaoka 1-6, Suita City, Osaka 565-0871, Japan.
E-mail:
nakagawa@phs.osaka-u.ac.jp

†These authors contributed equally to this work.

Received: 14 June 2004
Revised: 2 September 2004
Accepted: 2 September 2004

Abstract

Background PEGylation of adenovirus vectors (Ads) is an attractive strategy in gene therapy. Although many types of PEGylated Ad (PEG-Ads), which exhibit antibody evasion activity and long plasma half-life, have been developed, their entry into cells has been prevented by steric hindrance by polyethylene glycol (PEG) chains. Likewise, sufficient gene expression for medical treatment could not be achieved.

Methods A set of PEG-Ads, which have different PEG modification rates, was constructed, and gene expression was evaluated using A549 cells. A novel PEGylated Ad (RGD-PEG-Ad), which contained RGD (Arg-Gly-Asp) peptides on the tip of PEG, was developed. We evaluated gene expression both in Coxsackie-adenovirus receptor (CAR)-positive as well as -negative cells, and *in vivo* gene expression was also determined. Furthermore, the antibody evasion ability and the specificity of infection exhibited by this RGD-PEG-Ad were also evaluated.

Results Whereas PEG-Ads decreased gene expression in CAR-positive cells, RGD-PEG-Ad enhanced gene expression notably, to a level about 200-fold higher than that of PEG-Ads. Moreover, gene expression of RGD-PEG-Ad was almost equal to that of Ad-RGD, which contains an RGD-motif in the fiber and exhibits among the highest gene expression of CAR-positive and -negative cells. Furthermore, although Ad-RGD gene expression decreased remarkably in the presence of anti-Ad antiserum, RGD-PEG-Ad maintained its activity against antibodies. *In vivo* experiments also demonstrated that the modification of Ads with RGD-PEG induced efficient gene expression.

Conclusions In the present study, we demonstrated that a new strategy, which combined integrin-targeting the RGD peptide on the tip of PEG and modified the Ad using this material, could enhance gene expression in both CAR-positive and -negative cells. At the same time, this novel PEGylated Ad maintained strong protective activity against antibodies. This strategy could also be easily modified for developing other vectors using other targeting molecules. Copyright © 2004 John Wiley & Sons, Ltd.

Keywords adenovirus; antibody; polyethylene glycol; RGD peptide; gene expression

Introduction

Gene therapy for cancer or other incurable diseases has attracted considerable attention. The major obstacle to widespread utilization of gene therapy

involves the transgenic vector. Adenovirus vectors (Ads) exhibit high transduction efficiency and gene expression, and can efficiently transfer genes into both dividing and non-dividing cells. Therefore, they are widely used as vectors for gene therapy [1–4]. On the other hand, many people carry neutralizing antibodies to Ads, and the administration of a large amount of Ads may cause side effects. Therefore, clinical application of Ads is difficult [5,6], and many studies have been conducted in an attempt to overcome the limitations of Ads [7–9].

PEGylation, the covalent attachment of activated monomethoxy polyethylene glycol to free lysine groups on the surface of an Ad, is a promising strategy for overcoming these limitations. PEGylation of therapeutic proteins such as cytokines has been reported previously [10,11], and several groups have reported that PEGylated adenovirus exhibits several advantageous attributes [12–14]. Without the need for modifying Ad capsid protein by genetic recombination, a PEGylated Ad (PEG-Ad) can transduce its therapeutic gene into cells even in the presence of Ad-neutralizing antibodies [15,16], and extend residence time in the blood [17]. Furthermore, targeting of PEG-Ads has also been attempted. Lanciotti *et al.* reported targeting Ads using heterofunctional PEG, tresyl-PEG-maleimide [18]. Conjugation of optimized fibroblast growth factor 2 (FGF2), which possesses monoreactive cysteine, to the maleimide group on PEG-Ad was mediated by a reactive sulfhydryl group on the surface of the protein. Ogawara *et al.* reported enhanced transgene delivery to activated vascular endothelial cells using a PEG-Ad combined with an antibody on the tip of PEG [19]. These reports suggest that the use of a functional molecule on the tip of PEG can efficiently change the tropism of Ads or PEG-Ads.

In the present study, we attempted to overcome the previously observed reduction in gene expression caused by the inhibition of endocytosis through the Coxsackie-adenovirus receptor (CAR). This inhibition is due to steric hindrance by the PEG chains and has prevented the widespread therapeutic use of PEG-Ads. Therefore, we developed a new versatile Ad that maintained the positive attributes of PEGylation but also exhibited high transduction efficiency both in CAR-positive and -negative cells.

Infection by Ads occurs in two distinct steps. In the first step, the fiber protein of the Ad binds to its CAR [20–22], and the transduction efficiency of this step is influenced by the amount of CAR present. Following this, internalization via receptor-mediated endocytosis is promoted when the RGD motif of the penton bases combines with $\alpha v\beta 3$ and $\alpha v\beta 5$ integrins [23,24], which are present on many types of cells. We focused on the second step of Ad infection and constructed PEG with RGD peptides on the tip. The PEGylated Ad (RGD-PEG-Ad), which contained RGD peptide on the tip of PEG, was expected to show high transduction efficiency for both CAR-positive and -negative cells because of the interaction between RGD and integrin. Likewise, RGD-PEG-Ad possesses the ability to avoid neutralizing antibodies, a major advantage of PEGylation [15,16]. Incidentally, an Ad that contains an RGD peptide in the HI loop of the fiber (Ad-RGD) has already been developed, and this vector exhibits the highest transduction efficiency via integrin [25,26].

In the present study, we constructed several PEG-Ads at various PEG modification rates, and measured their gene expression. Following this, we used Lipofectamine to determine whether PEG-Ads possessed high gene expression ability. This verified that, upon entering a cell, PEG-Ad expressed the gene originating from the Ad itself. In the next step, we constructed RGD-PEG-Ad and measured its gene expression in CAR-positive and -negative cells with or without Ad antiserum.

Materials and methods

Cell lines

A549 (human lung carcinoma) cells were cultured in Dulbecco's modified Eagle's medium supplemented with 10% fetal calf serum (FCS). B16BL6 (mouse melanoma) cells were cultured in minimum essential medium supplemented with 7.5% FCS.

Development of adenovirus vectors

In this study, all experiments used E1-deleted Ad type 5, which expressed firefly luciferase under the control of cytomegalovirus (CMV) promoters. Both conventional and RGD fiber mutant Ads were amplified in 293 cells using a modification of established methods, purified from cell lysates by banding twice through CsCl gradients, dialyzed and stored at −80 °C. The Ads used in this study were constructed by an improved *in vitro* ligation method as described previously [27]. Determination of virus particle titer was accomplished spectrophotometrically by the methods of Maizel *et al.* [28].

Preparation of RGD-PEG

The synthetic scheme for RGD-PEG is shown in Figure 3. *N*-(9-Fluorenylmethoxycarbonyl)-*O*-(succimidyl)-ω-amino-α-carboxy-PEG (Fmoc-PEG-NHS, MW 3400) was purchased from Shearwater Corporation (USA). β-Ala (βA) was used as a spacer between PEG and the RGD peptide. (Ac-YGGRGDTPβA)$_2$K-PEG-βAC-amide (RGD-PEG, MW 5500) was synthesized manually on a Rink amide resin [29] using a 9-fluorenylmethoxycarbonyl (Fmoc)-based solid-phase strategy. We employed 2(1*H*-benzotriazol-1-yl)-1,1,3,3-tetramethyluronium hexafluorophosphate and 1-hydroxybenzotriazole as coupling reagents, trityl (Trt) protection as the sulfhydryl group source, *tert*-butyl as the hydroxyl group source and 2,2,5,7,8-pentamethylchroman-6-sulfonyl (Pmc) protection as the guanidinyl group source. To liberate the synthetic RGD-PEG from the resin, cleavage was achieved by using

a mixture of trifluoroacetic acid/triisopropylsilane/H_2O (95 : 2.5 : 2.5) [30] for 2 h at room temperature, followed by high-performance liquid chromatography (HPLC) purification on a C18 column. After addition of the peptide to *N*-(6-maleimidecaproyloxy)succinimide) (EMCS) in phosphate-buffered saline (PBS), pH 6.4, the solution was changed to pH 7.4 PBS and kept frozen at −80 °C.

Covalent attachment of PEG to Ads

Activated methoxypolyethylene glycol-succinimidyl propionate (mPEG-SPA, MW 5000; Shearwater Corporation, USA) and RGD-PEG were used in this study. Ads were reacted with 25–6400-fold molar excess of mPEG-SPA to viral lysine residue at 37 °C for 45 min with gentle stirring. Ads were also reacted with 250-fold molar excess of RGD-PEG under the same conditions. CsCl gradient ultracentrifugation was used for PEGylated adenovirus purification, and we assessed whether unmodified Ads were mixed with the PEGylated Ad. Modification ratio of PEGylated-Ads was determined by sodium dodecyl sulfate/polyacrylamide gel electrophoresis (SDS-PAGE) analysis using NIH image software. SDS-PAGE was carried out, referring to the previous report by O'Riordan *et al.* [15], in a 4–20% polyacrylamide gel (PAG Mini 4/20; Daiichi Pure Chemicals, Japan). Viral protein (hexon) was stained by Coomassie brilliant blue. The PEGylated hexon band was separated from the unmodified hexon band. The ratios of each band were measured using NIH Image software, and the PEG modification ratio was calculated as described below, the band of PEGylated hexon/the band of PEGylated and unmodified hexon ×100 [16]. After dilution in PBS, the particle sizes of Ads and RGD-PEG-Ad were measured using a Zetasizer 3000HS (Malvern Inc. UK).

Transduction efficiency of PEGylated Ads into A549 cells

A549 cells (2×10^4 cells/well) were seeded onto a 48-well plate. On the following day, the cells were transduced with 300, 1000, 3000, or 10 000 particles/cell of unmodified Ads and PEG-Ads that possessed various PEG modifications in a final volume of 500 µl in cell medium. After 24 h cultivation, luciferase activity was measured using the luciferase assay system (Promega, USA) and Microlumat Plus LB 96 (Perkin Elmer, USA) after cells had been lysed with the luciferase cell culture lysis reagent (Promega, USA). Luciferase activity was calculated as relative light units (RLU)/well. In the presence of 20 µg/ml Lipofectamine 2000 (Invitrogen, USA), A549 cells were transduced with 1000 particles/cell of unmodified Ads, 43%, 72%, and 89% modified PEG-Ads, heatinactivated Ads, or heat-inactivated PEG-Ads, respectively. After 4 h, the virus solution was replaced with fresh medium, and the cells were incubated for 24 h. Subsequently, luciferase expression was measured using the method described above.

Transduction efficiency of RGD-PEG-Ad into A549 and B16BL6 cells

A549 and B16BL6 cells (2×10^4 cells/well) were seeded onto a 48-well plate. On the following day, the cells were transduced with 300, 1000, 3000, and 10 000 particles/cell of unmodified Ads, PEG-Ads, RGD-PEG-Ad or Ad-RGD, respectively, in a final volume of 500 µl in cell medium. After 24 h cultivation, luciferase activity was measured using the method described above.

Competition experiments using RGD peptide

B16BL6 cells (2×10^4 cells/well) were seeded onto a 48-well plate. On the following day, cells were incubated with RGD peptide (GRGDTP, SIGMA) at a final concentration of 200 µg/ml for 10 min at room temperature, and then 3000 particles/cell of unmodified Ads, RGD-PEG-Ad or Ad-RGD were added to a final volume of 300 µl in cell medium. After 24 h cultivation, luciferase activity was measured using the method described above.

Preparation of Ad antiserum

Ad antiserum was obtained from ICR mice using methods previously reported by us and others [16,31]. In brief, a dose of 10^{10} particles of unmodified Ad containing Freund's complete adjuvant in 100 µl of PBS was administered hypodermically to a female ICR mouse (6 weeks old). Two to four weeks later, an additional dose of 10^{10} viral particles in Freund's incomplete adjuvant was hypodermically administered. Mouse serum was collected after 1 week, and stored at −20 °C.

Antibody evasion by RGD-PEG-Ad in B16BL6 cells

B16BL6 cells (2×10^4 cells/well) were seeded onto a 48-well plate. On the following day, the cells were transduced with 1000 particles/cell of RGD-PEG-Ad or Ad-RGD in a final volume of 500 µl in cell medium in the presence or absence of 100 µl/well Ad antiserum (42, 125 ng protein/well). After 24 h cultivation, luciferase activity was measured using the method described above.

Ad-mediated gene transduction *in vivo*

Unmodified Ad, Ad-RGD, and RGD-PEG-Ad (1.5×10^{10} particles/100 µl) were intravenously injected into BALB/c mice (female, 6 weeks old; obtained from Nippon SLC, Kyoto, Japan). Forty-eight hours later, organs were isolated and homogenized as previously described [32]. Luciferase activity was measured using the method described above.

Statistical analysis

Student's t-test was used for statistical comparison when applicable. Differences were considered statistically significant at $P \leq 0.05$.

Results

Transduction efficiency of Ads declines in response to PEGylation

We confirmed the feasibility of constructing PEG-Ads that exhibit various PEG modification rates, which are regulated by the amount of PEG made available for the reaction (data not shown). In the present study, Ads were reacted with 25-, 100-, 400-, 1600- and 6400-fold molar excesses of PEG relative to viral lysine residue. The results showed that the transduction efficiency of PEG-Ads fell remarkably as the PEG modification rate increased (Figure 1). Luciferase expression of the 34% modified PEG-Ad was approximately 200-fold lower than that of unmodified Ads, and gene expression of the 89% modified PEG-Ad fell by 100 000 or more and was not dose-dependent.

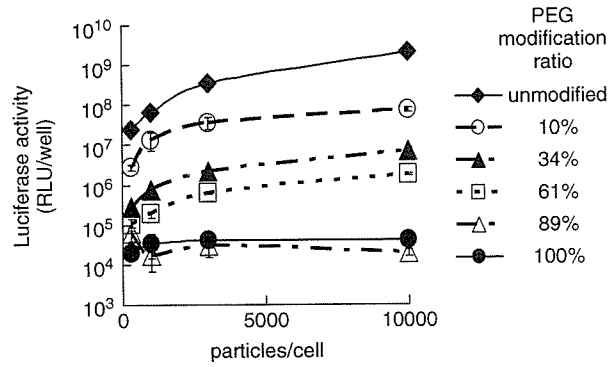

Figure 1. Transduction efficiency of PEGylated adenovirus vectors into A549 cells. A549 cells (2×10^4 cells) were transduced with 300, 1000, 3000 or 10 000 particles/cell of unmodified Ad or PEG-Ad encoding the luciferase gene at the indicated modification ratios. Luciferase expression was measured after 24 h. Each point represents the mean ± S.D. (n = 3)

PEG-Ads show high gene expression upon cell entry

We introduced PEG-Ads into cells using Lipofectamine and measured their gene expression in order to verify that the decrease of gene expression of PEG-Ads was derived from binding inhibition due to steric hindrance by PEG chains. The results shown in Figure 2 demonstrated that, in the absence of Lipofectamine, the transduction efficiency of PEG-Ads significantly decreased as PEG modification rate increased. However, in the presence of Lipofectamine, PEG-Ad gene expression at 43% modification was enhanced significantly to nearly that of unmodified Ads. Even at high modification rates (89%), the PEG-Ad gene expression in the presence of Lipofectamine was more than 130-fold higher than that in the absence of Lipofectamine. The gene expression of the heat-inactivated unmodified Ads and the heat-inactivated PEG-Ads were very low even with Lipofectamine. The results

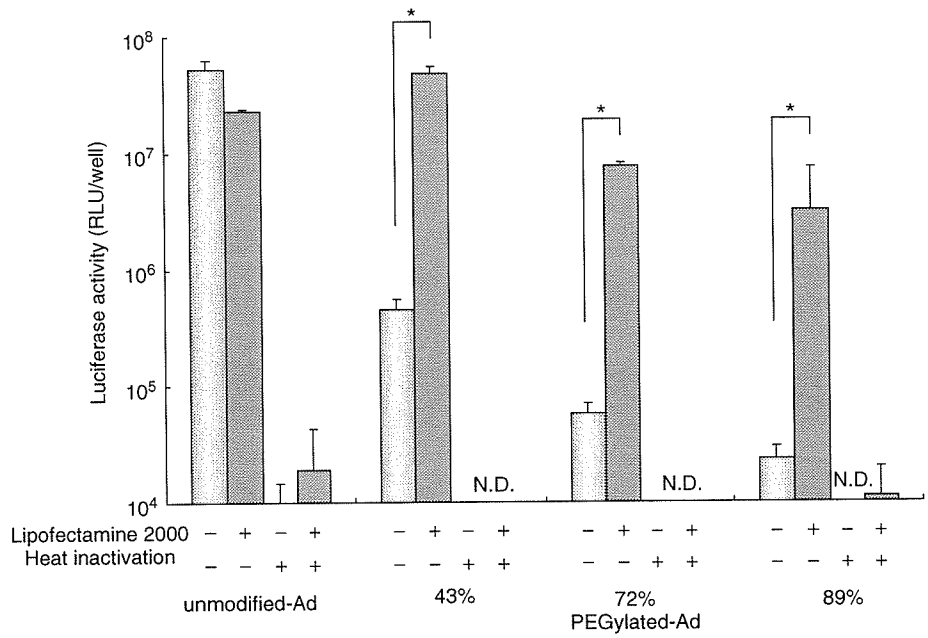

Figure 2. Transduction efficiency of PEGylated adenovirus vectors into A549 cells in the presence or absence of Lipofectamine 2000. A549 cells (2×10^4 cells) were transduced with 1000 particles/cell of unmodified Ad or PEG-Ad in the presence or absence of 20 μg/ml of Lipofectamine 2000. After 4 h, the virus solution was replaced with fresh medium, and the cells were incubated for 24 h. Luciferase expression was measured. Each point represents the mean ± S.D. (n = 3). *$P < 0.05$ (Student's t-test)

shown here indicate that high transduction efficiency, which is characteristic of Ads, decreased due to the steric hindrance of CAR by PEG chains.

Construction of PEGylated Ads with RGD peptides

In selecting the adhesion molecule, we focused on the RGD motif, the second mediator of Ad internalization. We constructed RGD-PEG-Ad using RGD-PEG-NHS (Figure 3), which contains two RGD motifs (YGGRGDTP) on the tip of PEG, and we investigated the characteristics of RGD-PEG-Ad (Table 1). RGD-PEG-Ad was 12.5 nm bigger in diameter than unmodified Ads, and the PEG modification rate (36%) was confirmed by SDS-PAGE and NIH Image software.

Enhanced transduction efficiency of RGD-PEG-Ad in comparison to that induced by PEG-Ads

We compared the transduction efficiency of unmodified Ads, PEG-Ads, Ad-RGD, and RGD-PEG-Ad in both A549 (CAR-positive) and B16BL6 (CAR-negative) cells. In A549 cells, RGD-PEG-Ad showed 100-fold higher gene expression than PEG-Ad, which exhibits the same level of modification. This gene expression level was similar to that of unmodified Ads and Ad-RGD (Figure 4A). In B16BL6 cells, RGD-PEG-Ad exhibited 60-fold and 200-fold higher gene expression rates than unmodified Ad and PEG-Ad, respectively, but the expression rate was similar to that of Ad-RGD (Figure 4B).

Table 1. Modification ratio and vectors size of RGD-PEG-Ad

Ratio (Ad/RGD-PEG)*	PEG modification ratio (%)	Vector size (nm)
1 : 0 (unmodified)	0	122.1 ± 4.5
1 : 250	36	134.6 ± 2.7

*Amount of PEG to lysine residue of adenovirus vector capsid protein (mol/mol)

RGD-PEG-Ad specifically infect cells through integrin

The specificity of RGD-PEG-Ad binding via integrin was evaluated by competition assay using the RGD peptide, GRGDTP, which has been widely used as a competitive peptide for integrin [33,34]. In the presence of GRGDTP, RGD-PEG-Ad and Ad-RGD gene expression was remarkably decreased compared to that in the absence of RGD peptide (Figure 5). In contrast, unmodified Ad did not decrease notably, suggesting the introduction of RGD-PEG-Ad was integrin-dependent.

RGD-PEG-Ad maintains its high gene expression in the presence of Ad antiserum

We evaluated transduction efficiency of Ad-RGD and RGD-PEG-Ad in the presence or absence of Ad antiserum using B16BL6 cells. In the presence of Ad antiserum, Ad-RGD gene expression was reduced remarkably. However, RGD-PEG-Ad maintained its high transduction efficiency (Figure 6). In the presence of 125 ng anti-Ad antibody,

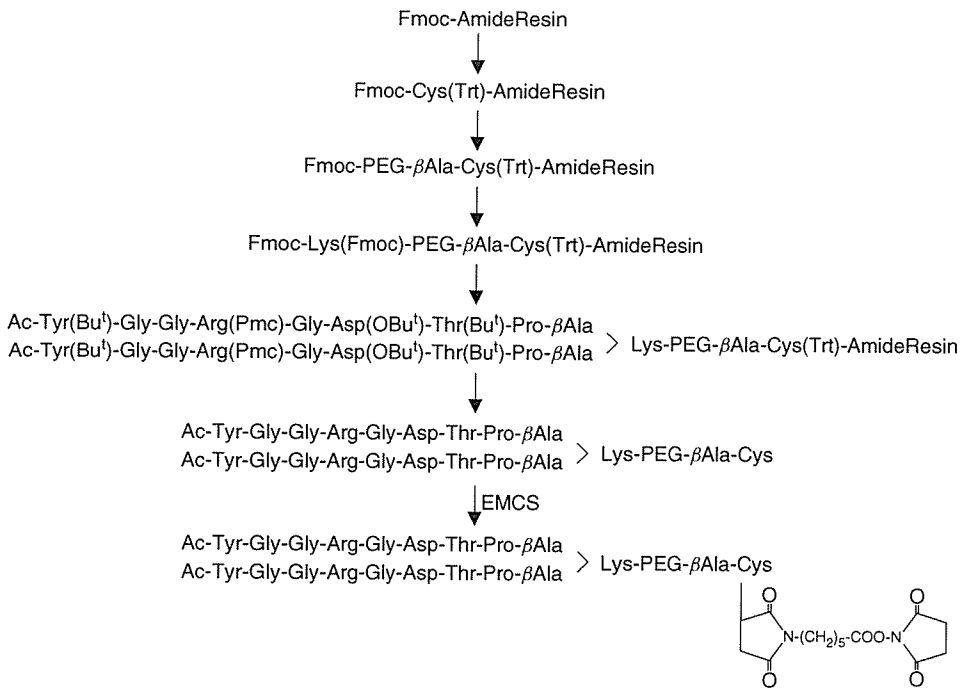

Figure 3. Structural scheme for RGD-PEG

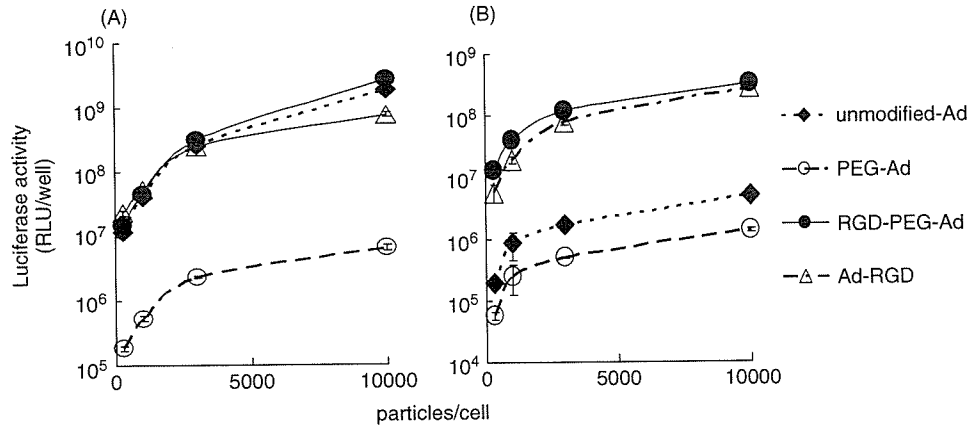

Figure 4. Transduction efficiency of RGD-PEGylated adenovirus vectors into A549 cells and B16BL6 cells. (A) A549 (2×10^4) cells and (B) B16BL6 cells (2×10^4) were transduced with 300, 1000, 3000 or 10 000 particles/cell of unmodified Ad, PEG-Ad, RGD-PEG-Ad or Ad-RGD, respectively. Luciferase expression was measured after 24 h. Each point represents the mean ± S.D. (n = 3)

RGD-PEG-Ad retained more than one-tenth of its activity, whereas Ad-RGD lost more than 99% of its activity in the absence of antibody.

RGD-PEG-Ad possessed high gene expression *in vivo*

Unmodified Ad, Ad-RGD, and RGD-PEG-Ad mediated luciferase activity predominantly in the liver after intravenous administration. No significant difference in liver transduction was found between unmodified Ad and RGD-PEG-Ad (Figure 7). Biodistribution of Ad-RGD and RGD-PEG-Ad was similar in lung, spleen, kidney, heart and brain (data not shown).

Discussion

Ads are widely used as vectors for gene therapy experiments. To date, several methods including gutless Ads, which address the decrease in antigenicity [35–37], and fiber mutant Ads [25,38,39], have been developed. In the present study, we initially focused on the modification of Ads by PEG because of its relative ease of development and many other merits such as evasion of neutralizing antibodies. However, as is well known, the conjugation of an Ad with high molecular weight material hinders its interaction with its receptor and subsequently influences the introduction of the virus. Therefore, our aim was to develop novel vectors that exhibit high gene expression while at the same time maintaining the other merits of PEGylated-Ads.

PEGylation of proteins and liposomes has already been widely employed and increased blood stability and mitigation of side effects have been reported [10,11]. PEGylation of the surface of Ads has several advantages. We and other groups have previously demonstrated that modification of an Ad with PEG protects it from neutralizing antibodies [15,16,31]. Likewise, PEGylation has been reported to extend the half-life of Ads in blood

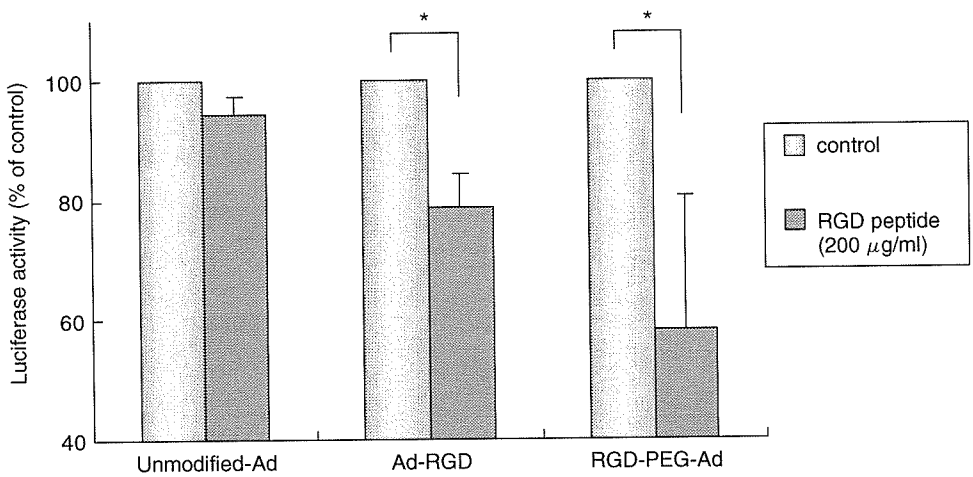

Figure 5. Transduction efficiency of RGD-PEGylated adenovirus vectors in the presence or absence of RGD peptide. B16BL6 cells (2×10^4) were transduced with 3000 particles/cell of unmodified Ad, Ad-RGD or RGD-PEG-Ad in the presence or absence of RGD peptide (200 μg/ml). Luciferase expression was measured after 24 h. Each point represents the mean ± S.D. (n = 3). *$P < 0.05$ (Student's t-test)

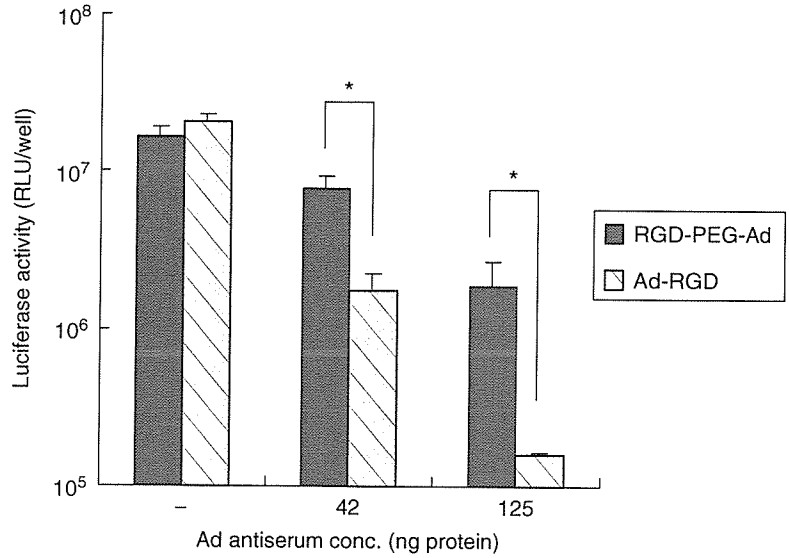

Figure 6. Transduction efficiency of RGD-PEGylated adenovirus vectors in the presence of adenovirus vector antiserum. B16BL6 cells (2×10^4) were transduced with 1000 particles/cell of RGD-PEG-Ad or Ad-RGD in the presence or absence of Ad antiserum. Luciferase expression was measured after 24 h. Each point represents the mean ± S.D. (n = 3). *$P < 0.05$ (Student's t-test)

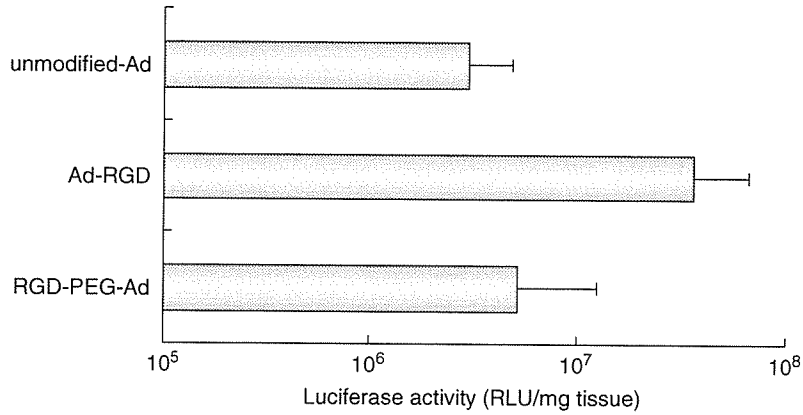

Figure 7. The gene expression in liver induced by RGD-PEG-Ad. 1.5×10^{10} particles of unmodified Ad, Ad-RGD, or RGD-PEG-Ad were injected intravenously. After 2 days, the liver was harvested and homogenized. Luciferase activity was then measured using the kit according to the manufacturer's instructions. Each point represents the mean ± S.D. (n = 4)

[17]. Steric hindrance by PEG chains and masking of the Ad surface electric charge were expected to reduce uptake by Kuppfer cells. In the present study, we established a method that can control the rate of Ad modification, and the results confirmed that PEGylation notably reduced gene expression efficiency in A549 cells. The data also suggest that increased modification with PEG induced lower gene expression (Figure 1).

In a clinical setting, the most serious problem associated with PEG-Ads is the decrease in transduction. We determined that this decrease results from the inhibition of Ad and CAR interaction due to steric hindrance by PEG chains (Figure 2). This suggests that high gene expression can be achieved if PEGylated-Ads can be transduced into cells. Therefore, in the present study, we focused on the RGD motif, which mediates the entrance of Ads into cells following the interaction with integrin [23,24]. We initially constructed RGD-PEG, which contains the RGD peptide at the tip of PEG, and reacted it with Ad to form RGD-PEG-Ad. The data in Table 1 demonstrate that the vector size of RGD-PEG-Ad was 12 nm bigger than that of unmodified Ad, and the same tendency was observed in the case of PEG-Ads. The size of Ads increased to about 10–15 nm at a PEG modification rate of 30–40% (data not shown). We thereby succeeded in developing a novel PEG-Ad, the efficacy of which was not influenced by the combination with PEG.

RGD-PEG-Ad gene expression in A549 cells was significantly higher than that of PEG-Ad, and was equivalent to conventional Ad and Ad-RGD (Figure 4). In CAR-negative B16BL6 cells, RGD-PEG-Ad also showed enhanced gene expression, which was much higher than that of PEG-Ads or conventional Ads. Because CAR is expressed at low levels in certain cells, such as hematopoietic stem cells, peripheral blood cells, differentiated airway epithelium, muscle cells, most mouse-derived cells, and many tumor cells, this novel PEGylated Ad is attractive for gene therapy. In addition,

our RGD-PEG-Ad was very stable under −80 °C storage conditions, despite several cycles of freezing and thawing (data not shown).

We also checked the specificity of RGD-PEG-Ad infection; we measured the gene expression of unmodified Ad, Ad-RGD, and RGD-PEG-Ad in the presence or absence of competitive RGD peptide (Figure 5). Koizumi *et al.* [25] have already reported the specificity of infection of Ad-RGD through integrin. In the present study, RGD-PEG-Ad gene expression was significantly inhibited by RGD peptide, GRGDTP, and, because RGD-PEG-Ad gene expression in CAR-negative, integrin-positive cells was notably enhanced compared to that of PEG-Ad, we suggest that the transduction of RGD-PEG-Ad was integrin-dependent.

Moreover, we determined whether RGD-PEG-Ad improved resistance to neutralizing antibodies (Figure 6). The expression of Ad-RGD genes fell remarkably in the presence of Ad antiserum. However, we demonstrated that RGD-PEG-Ad gene expression was far higher than that of Ad-RGD in the presence of the antiserum. This ability to evade antibodies is essential for clinical applications because nearly 80% of human patients possess anti-Ad antibodies, and re-administration is indispensable in some cases. Therefore, RGD-PEG-Ad minimizes the amount of medication required and reduces side effects.

The method described here is also applicable to other virus vectors and other target molecules. We are currently screening the use of peptides or antibodies as antigens or tissue-specific targeting molecules using the phage display system. These approaches will promote the development of a virus vector that exhibits enhanced safety and applicability.

Acknowledgements

This study was supported in part by the Research on Health Sciences focusing on Drug Innovation from The Japan Health Sciences Foundation; by Grants-in-Aid for Exploratory Research from the Ministry of Education, Culture, Sports, Science and Technology of Japan; and by grants from the Ministry of Health and Welfare in Japan.

References

1. Gao JQ, Tsuda Y, Katayama K, *et al.* Antitumor effect by interleukin-11 receptor alpha-locus chemokine/CCL27, introduced into tumor cells through a recombinant adenovirus vector. *Cancer Res* 2003; **63**: 4420–4425.
2. Crystal RG. Transfer of genes to humans: early lessons and obstacles to success. *Science* 1995; **270**: 404–410.
3. Wilson JM. Adenoviruses as gene-delivery vehicles. *N Engl J Med* 1996; **334**: 1185–1187.
4. Smith TA, Mehaffey MG, Kayda DB, *et al.* Adenovirus mediated expression of therapeutic plasma levels of human factor IX in mice. *Nat Genet* 1993; **5**: 397–402.
5. Wohlfart C. Neutralization of adenoviruses: kinetics, stoichiometry, and mechanisms. *J Virol* 1988; **62**: 2321–2328.
6. Mastrangeli A, Harvey BG, Yao J, *et al.* "Sero-switch" adenovirus-mediated in vivo gene transfer: circumvention of anti-adenovirus humoral immune defenses against repeat adenovirus vector administration by changing the adenovirus serotype. *Hum Gene Ther* 1996; **7**: 79–87.
7. Mizuguchi H, Koizumi N, Hosono T, *et al.* A simplified system for constructing recombinant adenoviral vectors containing heterologous peptides in the HI loop of their fiber knob. *Gene Ther* 2001; **8**: 730–735.
8. Yei S, Mittereder N, Tang K, *et al.* Adenovirus-mediated gene transfer for cystic fibrosis: quantitative evaluation of repeated in vivo vector administration to the lung. *Gene Ther* 1994; **1**: 192–200.
9. Croyle MA, Yu QC, Wilson JM. Development of a rapid method for the PEGylation of adenoviruses with enhanced transduction and improved stability under harsh storage conditions. *Hum Gene Ther* 2000; **11**: 1713–1722.
10. Tsutsumi Y, Tsunoda S, Kamada H, *et al.* Molecular design of hybrid tumour necrosis factor-alpha. II. The molecular size of polyethylene glycol-modified tumour necrosis factor-alpha affects its anti-tumour potency. *Br J Cancer* 1996; **74**: 1090–1095.
11. Yoshioka Y, Tsutsumi Y, Ikemizu S, *et al.* Optimal site-specific PEGylation of mutant TNF-alpha improves its antitumor potency. *Biochem Biophys Res Commun* 2004; **315**: 808–814.
12. Romanczuk H, Galer CE, Zabner J, *et al.* Modification of an adenoviral vector with biologically selected peptides: a novel strategy for gene delivery to cells of choice. *Hum Gene Ther.* 1999; **1**: 2615–2626.
13. Croyle MA, Chirmule N, Zhang Y, *et al.* "Stealth" adenoviruses blunt cell-mediated and humoral immune responses against the virus and allow for significant gene expression upon readministration in the lung. *J Virol* 2001; **75**: 4792–4801.
14. Croyle MA, Chirmule N, Zhang Y, *et al.* PEGylation of E1-deleted adenovirus vectors allows significant gene expression on readministration to liver. *Hum Gene Ther* 2002; **10**: 1887–1900.
15. O'Riordan CR, Lachapelle A, Delgado C, *et al.* PEGylation of adenovirus with retention of infectivity and protection from neutralizing antibody in vitro and in vivo. *Hum Gene Ther* 1999; **10**: 1349–1358.
16. Eto Y, Gao JQ, Sekiguchi F, *et al.* Neutralizing antibody evasion ability of adenovirus vector induced by the bioconjugation of MPEG-SPA. *Biol Pharm Bull* 2004; **27**: 936–938.
17. Alemany R, Suzuki K, Curiel DT. Blood clearance rates of adenovirus type 5 in mice. *J Gen Virol* 2000; **81**: 2605–2609.
18. Lanciotti J, Song A, Doukas J, *et al.* Targeting adenoviral vectors using heterofunctional polyethylene glycol FGF2 conjugates. *Mol Ther.* 2003; **8**: 99–107.
19. Ogawara K, Rots MG, Kok RJ, *et al.* A novel strategy to modify adenovirus tropism and enhance transgene delivery to activated vascular endothelial cells in vitro and in vivo. *Hum Gene Ther* 2004; **15**: 433–443.
20. Bergelson JM, Krithivas A, Celi L, *et al.* The murine CAR homolog is a receptor for coxsackie B viruses and adenoviruses. *J Virol* 1998; **72**: 415–419.
21. Tomko RP, Xu R, Philipson L. HCAR and MCAR: the human and mouse cellular receptors for subgroup C adenoviruses and group B coxsackieviruses. *Proc Natl Acad Sci U S A* 1997; **94**: 3352–3356.
22. Bewley MC, Springer K, Zhang YB, *et al.* Structural analysis of the mechanism of adenovirus binding to its human cellular receptor, CAR. *Science* 1999; **286**: 1579–1583.
23. Wickham TJ, Mathias P, Cheresh DA, Nemerow GR. Integrins alpha v beta 3 and alpha v beta 5 promote adenovirus internalization but not virus attachment. *Cell* 1993; **73**: 309–319.
24. Mathias P, Wickham T, Moore M, Nemerow G. Multiple adenovirus serotypes use alpha v integrins for infection. *J Virol* 1994; **68**: 6811–6814.
25. Koizumi N, Mizuguchi H, Hosono T, *et al.* Efficient gene transfer by fiber-mutant adenoviral vectors containing RGD peptide. *Biochim Biophys Acta* 2001; **1568**: 13–20.
26. Reynolds P, Dmitriev I, Curiel D. Insertion of an RGD motif into the HI loop of adenovirus fiber protein alters the distribution of transgene expression of the systemically administered vector. *Gene Ther* 1999; **6**: 1336–1339.
27. Mizuguchi H, Kay MA. Efficient construction of a recombinant adenovirus vector by an improved in vitro ligation method. *Hum Gene Ther* 1998; **9**: 2577–2583.
28. Maizel JV Jr, White DO, Scharff MD. The polypeptides of adenovirus. I. Evidence for multiple protein components in the

virion and a comparison of types 2, 7A, and 12. *Virology* 1968; **36**: 115–125.
29. Rink H. Solid-phase synthesis of protected peptide fragments using a trialkoxydiphenylmethyl ester resin. *Tetrahedron Lett* 1987; **28**: 3787–3790.
30. Sieber P. Modification of tryptophan residues during acidolysis of 4-methoxy-2,3,6-trimethylbenzenesulfonyl groups. *Tetrahedron Lett* 1987; **28**: 1637–1641.
31. Chillon M, Lee JH, Fasbender A, *et al.* Adenovirus complexed with polyethylene glycol and cationic lipid is shielded from neutralizing antibodies in vitro. *Gene Ther* 1998; **5**: 995–1002.
32. Xu ZL, Mizuguchi H, Ishii-Watabe A, *et al.* Optimization of transcriptional regulatory elements for constructing plasmid vectors. *Gene* 2001; **11**: 149–156.
33. Wu ZZ, Li P, Huang QP, *et al.* Inhibition of adhesion of hepatocellular carcinoma cells to basement membrane components by receptor competition with RGD- or YIGSR-containing synthetic peptides. *Biorheology* 2003; **40**: 489–502.
34. Bronson RA, Fusi F. Evidence that an Arg-Gly-Asp adhesion sequence plays a role in mammalian fertilization. *Biol Reprod* 1990; **43**: 1019–1025.
35. Hardy S, Kitamura M, Harris-Stansil T, *et al.* Construction of adenovirus vectors through Cre-lox recombination. *J Virol* 1997; **71**: 1842–1849.
36. Von Seggern DJ, Chiu CY, Fleck SK, *et al.* A helper-independent adenovirus vector with E1, E3, and fiber deleted: structure and infectivity of fiberless particles. *J Virol* 1999; **73**: 1601–1608.
37. Zou L, Zhou H, Pastore L, Yang K. Prolonged transgene expression mediated by a helper-dependent adenoviral vector (hdAd) in the central nervous system. *Mol Ther* 2000; **2**: 105–113.
38. Belousova N, Krendelchtchikova V, Curiel DT, Krasnykh V. Modulation of adenovirus vector tropism via incorporation of polypeptide ligands into the fiber protein. *J Virol* 2002; **76**: 8621–8631.
39. Nicklin SA, Von Seggern DJ, Work LM, *et al.* Ablating adenovirus type 5 fiber-CAR binding and HI loop insertion of the SIGYPLP peptide generate an endothelial cell-selective adenovirus. *Mol Ther* 2001; **4**: 534–542.

Oncogene (2005) 24, 3130–3140

www.nature.com/onc

Enhanced oncolysis by a tropism-modified telomerase-specific replication-selective adenoviral agent OBP-405 ('Telomelysin-RGD')

Masaki Taki[1], Shunsuke Kagawa[1,2], Masahiko Nishizaki[1], Hiroyuki Mizuguchi[3], Takao Hayakawa[3], Satoru Kyo[4], Katsuyuki Nagai[5], Yasuo Urata[5], Noriaki Tanaka[1] and Toshiyoshi Fujiwara*[,1,2]

[1]*Division of Surgical Oncology, Department of Surgery, Okayama University Graduate School of Medicine and Dentistry, Okayama 700-8558, Japan;* [2]*Center for Gene and Cell Therapy, Okayama University Hospital, Okayama 700-8558, Japan;* [3]*Division of Cellular and Gene Therapy Products, National Institute of Health Sciences, Tokyo 158-8501, Japan;* [4]*Department of Obstetrics and Gynecology, Kanazawa University School of Medicine, Kanazawa 920-8641, Japan;* [5]*Oncolys BioPharma, Inc., Tokyo 106-0031, Japan*

Replication-competent oncolytic viruses are being developed for human cancer therapy. We previously reported that an attenuated adenovirus (OBP-301, 'Telomelysin'), in which the hTERT promoter element drives expression of E1A and E1B genes linked with an IRES, could replicate in cancer cells, and causes selective lysis of cancer cells. We further constructed OBP-405 ('Telomelysin-RGD') that contains an RGD motif in the HI loop of the fiber knob. We examined whether OBP-405 could be effective in overcoming the limitations of OBP-301, specifically their inefficient infection into cells lacking the primary receptor, the coxsackievirus and adenovirus receptor (CAR). By flow cytometric analysis, H1299 (lung) and SW620 (colorectal) tumor cells showed high levels of CAR expression, whereas LN444 (glioblastoma), LNZ308 (glioblastoma), and H1299-R5 (lung) tumor cells were negative for CAR expression. A quantitative real-time PCR analysis demonstrated that fiber-modified OBP-405 infected more efficiently than OBP-301, although the intracellular replication rate of both viruses was consistent. The comparative antitumor effect of fiber-modified OBP-405 and unmodified OBP-301 for human cancer cells was evaluated *in vitro* by XTT assay as well as *in vivo* by using athymic mice carrying xenografts. OBP-405 had a profound oncolytic effect on human cancer cell lines compared to OBP-301, in particular on cells with low CAR expression. Intratumoral injection of 10^7 plaque-forming units of OBP-405 into CAR-negative H1299-R5 lung tumor xenografts in *nu/nu* mice resulted in a significant inhibition of tumor growth and long-term survival in all treated mice. Moreover, selective replication of OBP-405 in the distant, uninjected H1299-R5 tumors was demonstrated. Our results suggest that fiber-modified replication-competent adenovirus OBP-405 exhibits a broad target range by increasing infection efficiency, an outcome that has important implications for the treatment of human cancers.

Oncogene (2005) **24,** 3130–3140. doi:10.1038/sj.onc.1208460
Published online 21 February 2005

Keywords: RGD; adenovirus; telomerase; replication; gene therapy

Introduction

The optimal treatment for human cancer requires an improvement of therapeutic ratio to increase cytotoxic efficacy on the tumor cells and decrease that on the normal cells. This may not be an easy task because most of normal cells surrounding tumors are sensitive to the cytotoxic treatment. Thus, to establish reliable therapeutic strategies for human cancer, it is important to seek the genetic and epigenetic targets present only in cancer cells. The emerging fields of functional genomics and functional proteomics provide an expanding repertoire of clinically applicable targeted therapeutics (Kohn *et al.*, 2004). Telomerase is a ribonucleoprotein complex responsible for the addition of TTAGGG repeats to the telomeric ends of chromosomes (Greider and Blackburn, 1985; Collins and Mitchell, 2002), and contains the enzymatic subunit human telomerase reverse transcriptase (hTERT) (Nakamura *et al.*, 1997). The hTERT proximal promoter can be used as a molecular switch for the selective expression of target genes in tumor cells (Koga *et al.*, 2000; Komata *et al.*, 2001; Gu *et al.*, 2000, 2002), since almost all advanced human cancer cells express telomerase and most normal cells do not (Kim *et al.*, 1994; Shay and Wright, 1996). Genetically modified adenoviruses have emerged as a new biological anticancer agent (McCormick, 2001; Fang and Roth, 2003). We previously constructed an adenovirus vector (OBP-301, 'Telomelysin'), in which the hTERT promoter element drives expression of E1A and E1B genes linked with an internal ribosome entry site (IRES), and showed that OBP-301 induced selective

*Correspondence: T Fujiwara, Center for Gene and Cell Therapy, Okayama University Hospital, 2-5-1 Shikata-cho, Okayama 700-8558, Japan; E-mail: toshi_f@md.okayama-u.ac.jp
Received 17 August 2004; revised 22 November 2004; accepted 15 December 2004; published online 21 February 2005

E1A and E1B expression in human cancer cells, but not in normal cells (Kawashima *et al.*, 2004). Therefore, OBP-301 can replicate and lyse only cancer cells, but not normal cells. In addition, OBP-301 will infect neighboring cancer cells, and induce oncolysis throughout the whole tumor mass *in vivo*.

Infection efficiency of the presently available adenoviral agent, which is derived from human adenovirus serotype 5, varies widely depending on the expression of Coxsackie-adenovirus receptor (CAR) (Wickham *et al.*, 1993). The initial step of adenovirus infection involves at least two sequential steps. The first step is the attachment of the virus to the cell surface through binding of the knob domain of the fiber to CAR (Bergelson *et al.*, 1997). Following attachment, the viral internalization into the cells occurs by the interaction of RGD (Arg-Gly-Asp) motifs of penton base with integrin receptors, $\alpha v\beta 3$ and $\alpha v\beta 5$, expressed on most cell types (Wickham *et al.*, 1993). Therefore, the interaction of the fiber knob with CAR on the cell is the key mediator by which adenoviral agents enter the cells. Modification of fiber protein is an attractive strategy for overcoming the limitations imposed by the CAR dependence of adenovirus infection (Wickham *et al.*, 1997; Dmitriev *et al.*, 1998; Krasnykh *et al.*, 1998; Mizuguchi *et al.*, 2001).

We modified the fiber of OBP-301 to contain RGD peptide, which binds with high affinity to integrins ($\alpha v\beta 3$ and $\alpha v\beta 5$) on the cell surface, on the HI loop of the fiber protein. The resultant adenovirus, termed OBP-405 or 'Telomelysin-RGD', mediated not only CAR-dependent virus entry but also CAR-independent, RGD-integrin ($\alpha v\beta 3$ and $\alpha v\beta 5$)-dependent virus entry. We explored whether OBP-405 containing RGD peptide on the fiber knob had more oncolytic efficacy on several types of human cancer cells (CAR-positive or -negative), as compared with OBP-301 containing wild-type fiber *in vitro* and *in vivo*.

Results

Expression of CAR and integrins in human cancer and normal cells

To investigate the antitumor effect of the fiber-modified OBP-405, we used several human cell lines. We first examined the expression levels of CAR and αv integrin family, $\alpha v\beta 3$ and $\alpha v\beta 5$, on each cell surface by flow cytometric analysis (Figure 1). Apparent amounts of CAR expression were detected on H1299 and SW620 cells, whereas LN444, LNZ308, and H1299-R5 cells expressed extremely low levels of CAR. The normal human lung fibroblast (NHLF) cell also exhibited detectable CAR expression. In contrast to CAR, $\alpha v\beta 3$ and $\alpha v\beta 5$ integrins were readily expressed in all cell lines.

Increased infection efficiency and selective replication of OBP-405

To assess whether incorporation of an RGD motif into the HI loop of the fiber knob domain would enhance its infectivity, CAR-positive parental H1299, CAR-negative LN444, and NHLF (normal cell) were infected with OBP-301 or OBP-405 at an multiplicity of infection (MOI) of 1. Quantitative real-time PCR analysis with DNA extracted 2 h after infection demonstrated that the amount of E1A DNA after OBP-405 infection was higher than that after OBP-301 infection in two human cancer cell lines, whereas infectivity of both viruses was almost similar in NHLF (Figure 2a). These results suggest that RGD-modified OBP-405 showed increased infectivity to neoplastic cells regardless of the levels of CAR expression, although the infectivity enhancement was greater in CAR-negative cancer cells.

We next examined the replication ability of OBP-301 and OBP-405 in different cell lines by measuring the relative amounts of E1A DNA. H1299, LN444, and NHLF cells were harvested at the indicated time points over 72 h after infection with OBP-301 or OBP-405, and subjected to quantitative real-time PCR analysis. The ratios were normalized by dividing the value of cells obtained 2 h after viral infection. As shown in Figure 2b, both OBP-301 and OBP-405 replicated 5–6 logs by 72 h after infection; their replication, however, were attenuated up to 3 logs in normal NHLF cells.

Enhanced viral spread of OBP-405 in human cancer cells

To examine whether increased infectivity of OBP-405 could facilitate viral spread, H1299, LN444, and NHLF cells cultured in chamber slides were infected either with OBP-301 or OBP-405 at an MOI of 1, and then immunohistochemically stained for viral hexon at 24 and 48 h of postinfection. Viral hexon was detectable in H1299 cells infected with OBP-301 and OBP-405 in a time-dependent manner, although the amount of positive cells after OBP-405 infection was higher than that after OBP-301 infection (Figure 3a). In contrast, viral hexon was only present in CAR-negative LN444 cells infected with OBP-405, but not in OBP-301-infected LN444 cells (Figure 3b), suggesting the selective replication of OBP-405 in CAR-negative human cancer cells. NHLF human normal cells exhibited no hexon-positive cells after OBP-301 or OBP-405 infection (Figure 3c).

In vitro *cytopathic efficacy of OBP-405 in CAR-negative human cancer cells*

To test whether the increased infectivity and replication of OBP-405 translated to improved oncolysis, we compared the cytopathic effect of OBP-405 with that of OBP-301 on various human cell lines *in vitro* (Figure 4). Both OBP-301 and OBP-405 killed CAR-positive H1299 and SW620 human cancer cells in a dose-dependent manner; OBP-405 at an MOI of 0.1, however, killed these cells as efficiently as OBP-301 at an MOI of 1, suggesting that OBP-405 showed approximately 10-fold more profound tumor cell killing compared with OBP-301. In contrast, only OBP-405 was lytic in CAR-negative LN444, LNZ308, and H1299-R5 cells, likely due to the higher infectivity of OBP-405

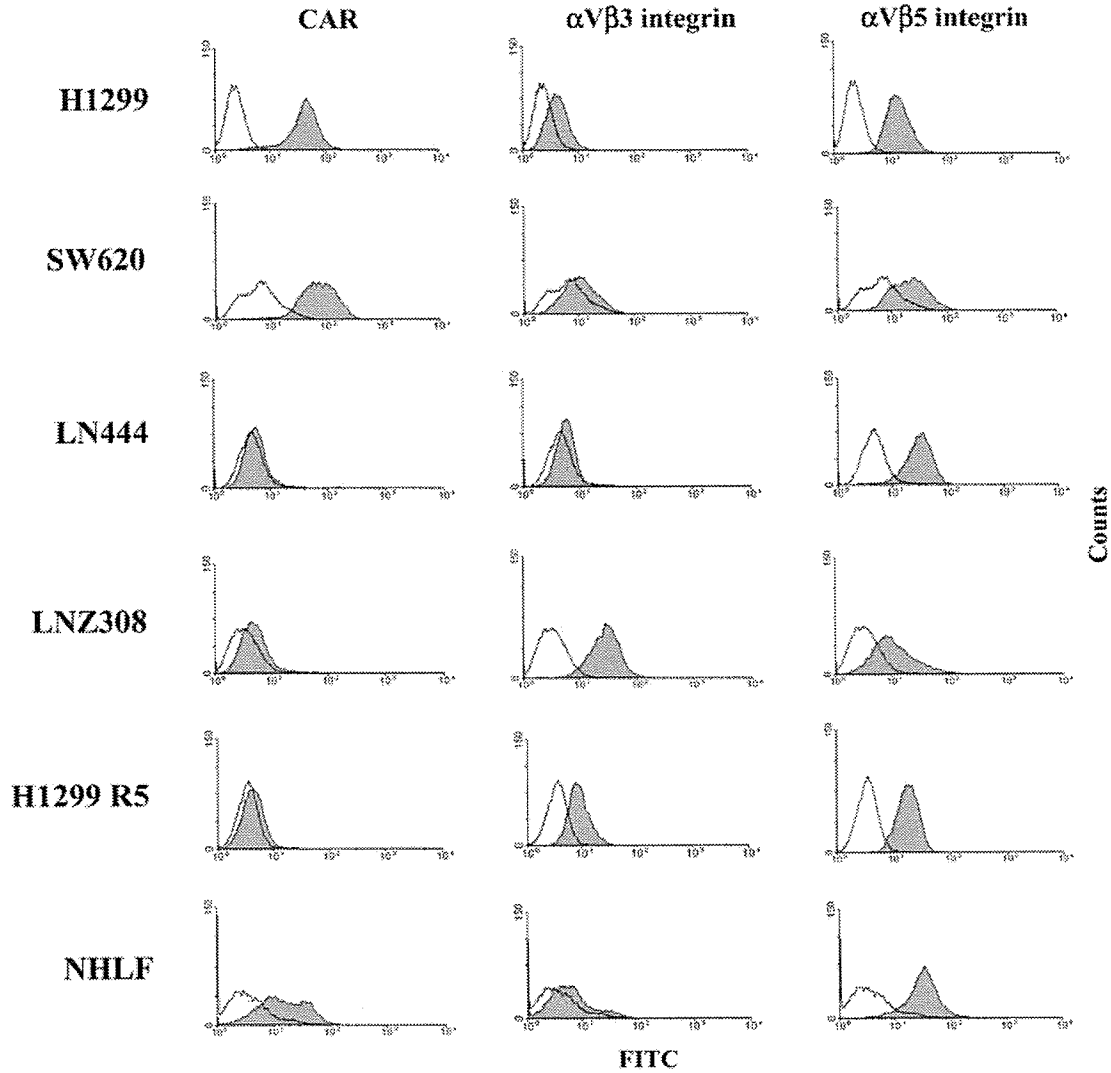

Figure 1 Flow cytometric analysis of CAR and integrin ($\alpha v\beta 3$ and $\alpha v\beta 5$) expression in human cancer and normal cell lines. Cells were incubated with anti-CAR (RmcB), anti-$\alpha v\beta 3$ integrin (LM609), and anti-$\alpha v\beta 5$ integrin (P1F6) monoclonal antibodies, followed by detection with FITC-labeled goat anti-mouse IgG secondary antibody. An isotype-matched normal mouse IgG1 conjugated to FITC was used as a control in all experiments (solid line)

in these cell lines. Most of these cells were dead within 5 days after OBP-405 infection, whereas OBP-301-infected cells were still intact at 5 days postinfection (Figure 4b). Neither OBP-301 nor OBP-405 exhibited cytopathic effect on NHLF cells.

Enhanced oncolysis of CAR-negative tumor xenografts by OBP-405

We next examined whether OBP-405 cause enhanced oncolysis and spread *in vivo*. Subcutaneous H1299-R5 tumor xenografts with a diameter of 5–6 mm received three daily courses of intratumoral injection of 1×10^7 plaque-forming units (PFU) of OBP-301, OBP-405 or replication-deficient control adenovirus (dl312), or PBS (mock). As shown in Figure 5, administration of OBP-405 resulted in significant growth suppression compared to mock- or dl312-treated tumors 34 days after virus injection ($P<0.01$). In addition, one of the six mice treated with OBP-405 showed the complete eradication of the established H1299-R5 tumor. We previously reported that intratumral injection of OBP-301 significantly inhibited the growth of H1299 tumor xenografts; a modest, insignificant growth inhibition, however, occurred with administration of OBP-301 on H1299-R5 tumors. Treatment with replication-deficient dl312 had no apparent effect on the growth of H1299-R5 tumors.

Targeting replication of OBP-405 in tumor tissues in vivo

To evaluate selective replication of OBP-301 and OBP-405 *in vivo*, we examined mouse tissues including implanted tumors for the presence of viral DNA and protein by quantitative real-time PCR and immunohistochemistry, respectively, following intratumoral viral

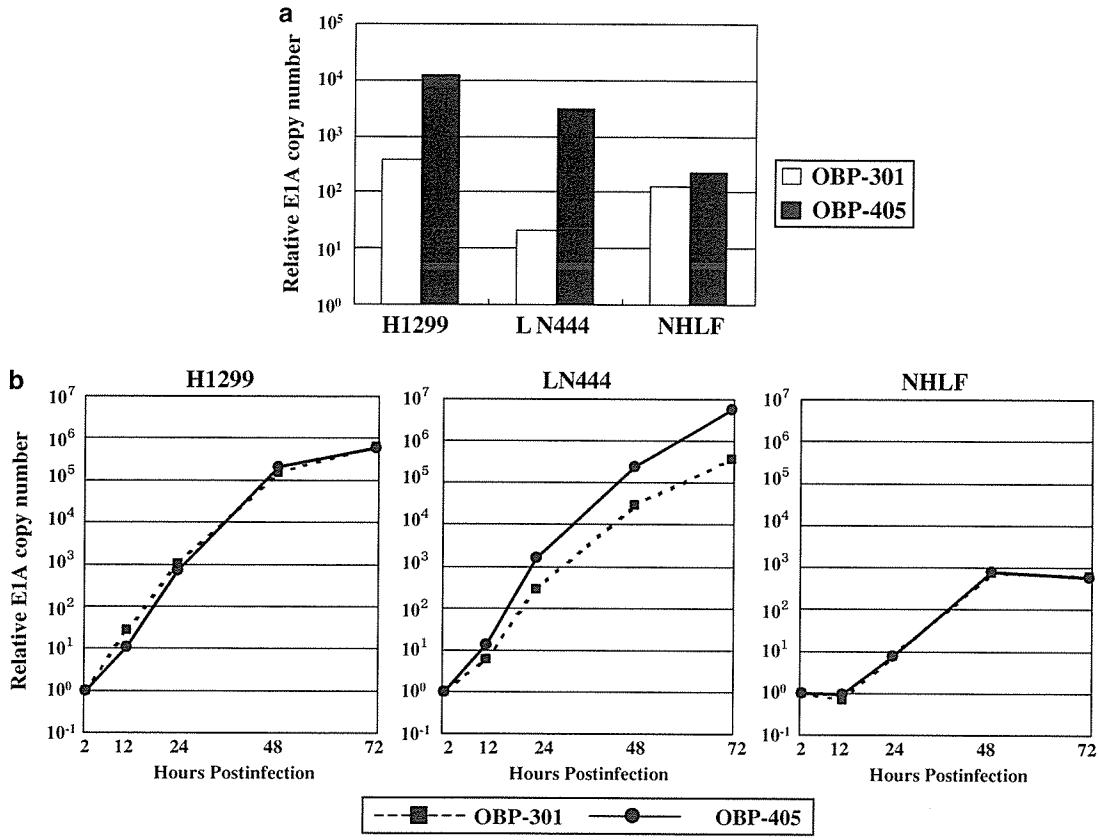

Figure 2 (**a**) Comparative analysis of the infection efficiency with OBP-301 and OBP-405 in H1299 (CAR-positive lung cancer), LN444 (CAR-negative glioblastoma), and NHLF (normal fibroblast) cells. Cells were infected with either OBP-301 or OBP-405 at an MOI of 1 for 2 h, and the viral infection rate was evaluated by measuring the E1A copy number using the real-time quantitative PCR method. (**b**) Assessment of viral DNA replication in H1299, LN444, and NHLF cells. Cells were infected with either OBP-301 or OBP-405 at an MOI of 1 for 2 h. Following the removal of virus inocula, cells were further incubated for the indicated periods of time, and then subjected to the real-time quantitative PCR assay. The amounts of viral E1A copy number are defined as the fold increase for each sample relative to that at 2 h (2 h equals 1)

injection. Mice with established subcutaneous H1299-R5 tumors received three daily courses of intratumoral injection of 1×10^7 PFU of OBP-301 or OBP-405, or PBS (mock), and killed 7 days after treatment. E1A DNA was not detected in any normal tissues examined (liver, kidney, pancreas, and spleen), however, it was apparently detected in tumors (Figure 6a). Tumors from mice treated with OBP-405 contained 100-fold more E1A DNA than tumors from OBP-301-treated mice (Figure 6a). Immunohistochemical staining of adenoviral hexon protein revealed that OBP-405 mediated viral spread throughout the tumor tissues that was less evident in OBP-301-treated animals (Figure 6b). In other normal organs, adenoviral hexon protein was absent (data not shown).

To directly address whether OBP-405 is not toxic, we measured levels of liver enzymes as an indicator of hepatocellular damages 7 days after intratumoral injection of 1×10^7 PFU of viruses. As shown in Table 1, no significant elevation of liver enzymes was observed in mice intratumorally injected with OBP-301 or OBP-405. In addition, histopathological analysis of liver sections demonstrated that there were no apoptotic hapatocytes or other histological signs of hapatocellular damages in mice treated with either OBP-301 or OBP-405 (data not shown).

Viral spread of OBP-405 in distant tumor tissues after intratumoral injection

We finally tested whether intratumoral injection of OBP-405 could mediate a therapeutic benefit on distant, uninjected H1299-R5 tumors in a dual tumor model. H1299-R5 tumors were established in the flanks at both left and right sides of *nu/nu* mice and viral replication in the left tumors was assessed after intratumoral inoculation of 1×10^7 PFU of either OBP-301 or OBP-405 into tumors in the right flank. Quantitative real-time PCR analysis on postinfection day 14 demonstrated that OBP-405 caused approximately 100-fold more efficient replication than OBP-301 in H1299-R5 tumors injected with viruses, whereas only OBP-405 replicated on distant, uninjected H1299-R5 tumors (Figure 7a).

At four weeks after viral injection, OBP-301 also replicated in uninjected H1299-R5 tumors; OBP-405, however, resulted in an approximately 100-fold more replication at uninjected sites (Figure 7b). In contrast,

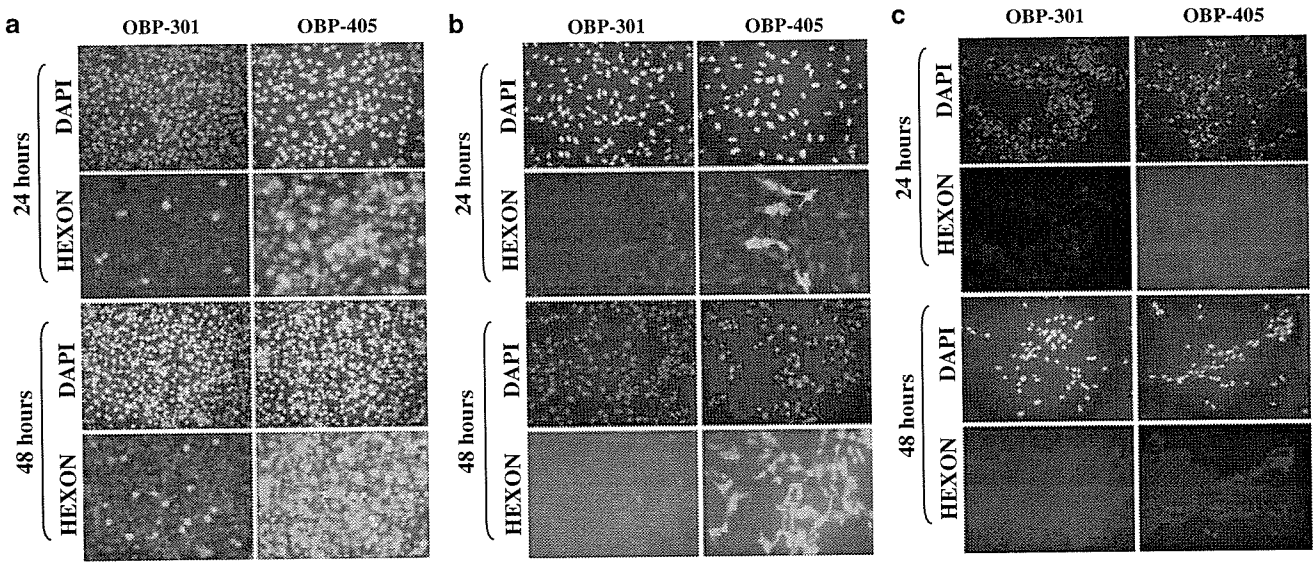

Figure 3 *In vitro* virus spread in CAR-positive H1299 **(a)**, CAR-negative LN444 **(b)**, and NHLF **(c)** cells. Cells cultured in chamber slides were infected with OBP-301 or OBP-405 at an MOI of 1. Cells stained with FITC-labeled goat anti-hexon antibody to monitor the replication of viruses 24 and 48 h after infection are shown. Cell nuclei were counterstained with DAPI. Virus replication was assessed with fluorescence microscopy, and the blue and green fluorescence correspond to cell nuclei and adenovirus hexon, respectively. Original magnification, ×200

H1299-R5 tumor treated with OBP-405 had completely disappeared, and the level of E1A copy number of OBP-301 was almost consistent with that at 14 day postinfection. These results suggest that OBP-405 could more efficiently replicate in both injected and uninjected tumors, when CAR-negative H1299-R tumors were treated. Notably, no E1A DNA could be detected in the blood of mice treated with OBP-301 or OBP-405, indicating that viral replication in tumors dose not correlate with the level of viruses in the blood circulation (Figure 7a and b).

Moreover, we histologically confirmed a profound replication of OBP-405 in untreated H1299-R5 tumors. As shown in Figure 7c, immunohistochemical analysis for the detection of adenoviral hexon demonstrated that the percentage of positive-staining cells was apparently higher in uninjected tumors of OBP-405-treated mice than those of OBP-301-treated mice. Hematoxylin/eosin analysis revealed apparent tumor cell death at the central portions of the tumors; morphological changes, however, that are associated with the apoptotic phenotype such as nuclear fragmentation and chromatin condensation were not evident (data not shown), suggesting that oncolysis by viral replication might be nonapoptotic cell death.

Discussion

Viral replication generally results in tissue destruction. Oncolytic viruses have been developed as an anticancer agent, because controlled replication in the tumors causes selective killing of tumor cells and minimizes the undesired effects on normal cells (Kirn *et al*., 2001). Amplified viruses can infect adjacent tumor cells as well as reach distant metastatic tumors with the blood circulation. Therefore, oncolytic viruses can amplify the administered dose as a result of *in vivo* viral replication. This might be one of the potential advantages of oncolytic viruses compared with conventional cancer therapies. We previously reported that hTERT promoter-specific replication-competent adenovirus OBP-301 could replicate and eventually lyse the telomerase-expressing tumors cells, leading to the viral spread to adjacent cells (Kawashima *et al*., 2004). OBP-301 could infect both normal and tumor cells, but the virus would only replicate in those cells that have robust telomerase activity. OBP-301 induced oncolysis in a variety of human cancer cell lines; tumors that lost CAR expression, however, might be refractory to infection with OBP-301, because subgroup C adenoviruses, including serotypes 2 and 5, rely on CAR as the primary binding

Figure 4 Oncolytic effect of OBP-301 and OBP-405 *in vitro* on human cancer and normal cell lines. **(a)** CAR-positive (H1299 and SW620) and CAR-negative (LN444, LNZ308, and H1299-R5) cell lines and normal cells (NHLF) were stained with Coomassie brilliant blue 5 day after infection with OBP-301 or OBP-405. Blue areas indicate viable cells; white areas show loss of cells through cell lysis. **(b)** Cells were infected with OBP-301 or OBP-405 at the indicated MOI values, and surviving cells were quantitated over 5 days by XTT assay. Statistical analysis was performed using Student's *t*-test for differences among groups. Statistical significance (*) was defined as $P<0.01$

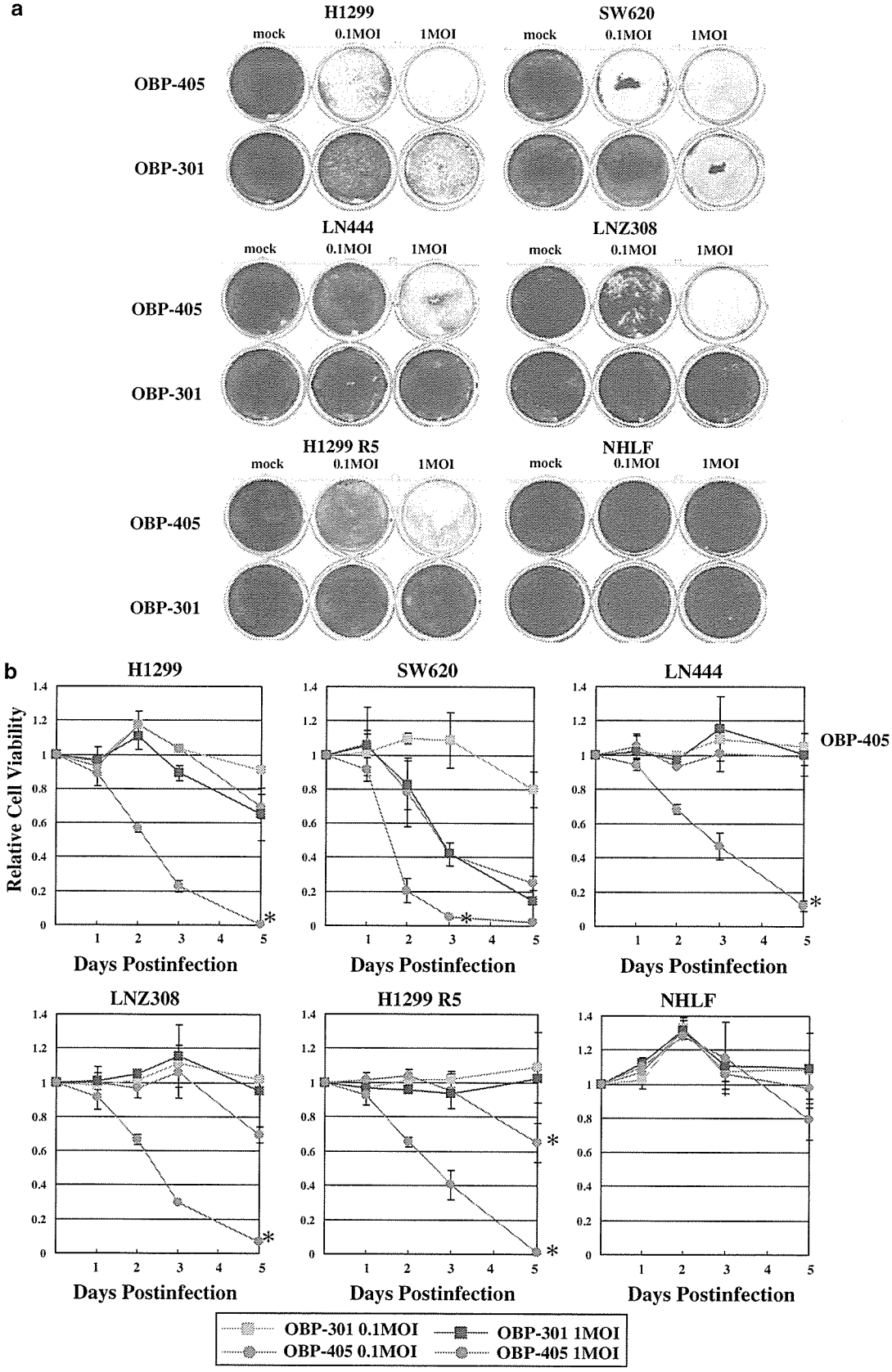
a
H1299
SW620
LN444
LNZ308
H1299 R5
NHLF
mock
0.1MOI
1MOI
OBP-405
OBP-301
b
Relative Cell Viability
Days Postinfection
OBP-405
OBP-301 0.1MOI
OBP-301 1MOI
OBP-405 0.1MOI
OBP-405 1MOI

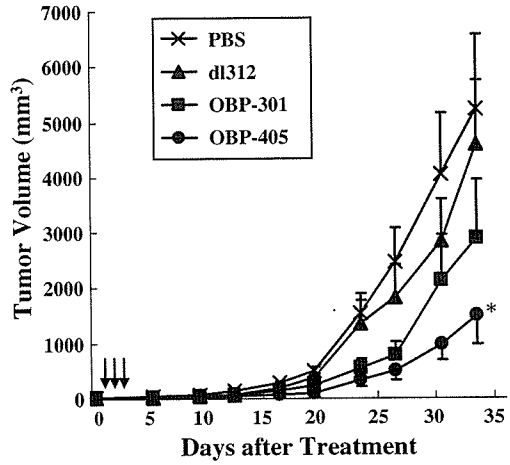

Figure 5 Antitumor effects of intratumorally injected OBP-301 or OBP-405 against established flank H1299-R5 xenograft tumors in *nu/nu* mice. PBS and replication-deficient dl312 were used as a control. Six mice were used for each group. The tumor growth was expressed by the tumor mean volume ±s.e. Statistical significance (*) was defined as $P<0.01$ (Student's *t*-test)

site on the target cells (Bergelson *et al.*, 1997). In fact, CAR deficiency in primary tumors has been reported (Miller *et al.*, 1998; Li *et al.*, 1999). Here, we demonstrate that the modification of the adenovirus fiber knob by the addition of an RGD-containing peptide in the HI loop increased its infectious efficiency and enabled the virus to kill CAR-negative tumor cells. The fiber-modified new oncolytic adenovirus OBP-405 was more effective to inhibit the growth of CAR-negative tumors *in vivo*, comprised of OBP-301.

A wide spectrum of CAR levels exists among many types of human cancer lines (Figure 1), although the regulation as well as the function of this transmembrane protein are poorly understood. If expression of CAR on target cells could be increased, this could potentially yield improved efficacy of adenovirus-based therapies. We previously established H1299-R5 human lung cancer cell line refractory to adenovirus infection by five-time repeated infections (Tango *et al.*, 2004). The observation that CAR expression markedly diminished as the cells are repeatedly infected with adenovirus suggests that the levels of CAR expression could be altered. Indeed, It has been reported that the chemotherapeutic agents are effective in increasing CAR expression (Hemminki *et al.*, 2003); in our preliminary experiments, however, CAR expression could not be modified in H1299-R5 cells by any chemotherapeutic agents tested, including the EGF receptor-tyrosine kinase inhibitor ZD1839 (Gefitinib, 'Iressa') (data not shown). Therefore, it seems to be difficult to consistently upregulate CAR expression in various types of human cancer cells.

A variety of strategies have been devised to increase adenovirus infection to cells with low or absent CAR. For our study, we have chosen to alter the tropism of oncolytic virus by the modification of the fiber. Making the fiber-modified oncolytic adenovirus, we supposed that the virus could infect not only by CAR-dependent entry but also by CAR-independent, RGD-integrin ($\alpha v\beta 3$ and $\alpha v\beta 5$)-dependent entry. As expected, OBP-405 was taken up efficiently by both CAR-positive and CAR-negative human cancer cells; the infectivity of OBP-405 was 10- and 1000-fold higher in CAR-positive and CAR-negative human cancer cell lines, respectively, than that of OBP-301 (Figure 2a). In contrast, the replication yields of OBP-301 and OBP-405 were persistent in both cell lines (Figure 2b), indicating that the tropism modification is not anticipated to alter fundamental aspects of the viral replication cycle. The increased initial virus entry into the cells results in earlier detection (data not shown) and augmented yields of OBP-405 compared with unmodified OBP-301 (Figure 3). Enhancing the infection efficiency of OBP-405 translated into increased oncolytic effects (Figure 4). OBP-301 showed complete oncolysis at as low as 1 MOI in H299 and SW620 cells, suggesting that OBP-301 is sufficient to treat CAR-positive human cancer cells; OBP-301, however, could not kill CAR-negative cell lines at all. Notably, OBP-405 did effectively kill LN444, LNZ308, and H1299-R5 cells at an MOI of 1, indicating that the infection enhancement of OBP-405 contributed to its efficacy on CAR-negative cancer cells. Another important finding is that OBP-405 elicited no increased infectivity as well as cytopathic effect to normal cells despite of CAR expression (Figures 3 and 4).

We also demonstrated the superior oncolytic effect of OBP-405 in the subcutaneous xenograft model of CAR-negative H1299-R5 cells. Intratumoral injection of OBP-405 for three consecutive days resulted in the significant inhibition of H1299-R5 tumor growth (Figure 5) and selective spread of viruses throughout the tumor tissues (Figure 6b). Although the RGD fiber knob modification of selectively replicating adenoviruses, such as AdΔ24 containing the Rb-binding mutation in E1A (Lamfers *et al.*, 2002) and the cyclooxygenase-2 (Cox-2) promoter-based adenovirus (Davydova *et al.*, 2004), has been previously reported to reduce tumor size *in vivo*, the major advantage of OBP-405 is the broad applicability for many types of human cancers because of the telomerase-specific hTERT promoter. In fact, many studies have reported that telomerase is present in nearly all immortal cell lines and ~90% of human tumors but seldom in normal somatic cells (Kim *et al.*, 1994; Shay and Wright, 1996). In addition to the antitumor effect, when the tropism of the virus is modified, it has to be addressed whether a pattern of biodistribution could be affected. We observed that OBP-405 showed a tumor-restricted pattern of biodistribution in mice after intratumoral administration (Figure 6a) and no hepatotoxicity despite of high levels of CAR and αv integrin expression in the liver (Tomko *et al.*, 1997; Fechner *et al.*, 2000) (Table 1). Viral replication and spread of OBP-405 could be detected at least for 4 weeks (Figure 7b), whereas OBP-405 was negative in any normal specimen throughout the period (data not shown). A limitation of our biodistribution data is that the hTERT promoter is not expected to function in mice as it does in humans. Indeed, some studies have reported that mouse and rat tumors do not support efficient replication of human